The Theory of Intrinsic Energy

Donald H. MacAdam
dhmintrinsic@gmail.com

Abstract

The assumption that all energy is kinetic has resulted in important phenomena with unknown mechanisms: stellar rotation curves, increase in mass with increase in velocity, constancy of photon velocity, and the levitation, suspension and pinning of superconducting disks. In addition, the reason for the existence of the fine structure constant is unknown, the value of the proton-electron mass ratio is unexplained, the spectra of atoms larger than hydrogen cannot be derived, and there is no proof or disproof of cosmic inflation. All of the above issues are resolved by the existence of intrinsic energy.

Contents

Part One “Gravitation and the fine structure constant” derives the fine structure constant, the proton-electron mass ratio, and the mechanisms of gravitation including non-Newtonian stellar rotation curves and the non-Newtonian precession rate of the perihelion of mercury.

Part Two “Structure and chirality” describes the structure of particles and the chirality meshing interactions that mediate action at a distance between particles and gravitons (gravitation) and particles and quantons (electromagnetism) and describes the properties of photons (with the mechanisms of diffraction and constant photon velocity).

Part Three “Nuclear magnetic resonance” is a derivation of the gyromagnetic ratios and nuclear magnetic moments of 106 isotopes.

Part Four “Particle acceleration” derives the mechanism for the increase in mass (mass-energy) in particle acceleration.

Part Five “Atomic Spectra” reformulates the Rydberg equations for the spectral series of hydrogen, and derives the atomic spectra of helium, lithium, beryllium, and boron.

Part Six “Cosmology” disproves cosmic inflation.

Part Seven “Magnetic levitation and suspension” quantitatively explains the levitation of pyrolytic carbon, and the levitation, suspension and pinning of superconducting disks.

Part One

Gravitation and the fine structure constant

"That gravity should be innate inherent & essential to matter so that one body may act upon another at a distance through a vacuum without the mediation of anything else by & through which their action or force may be conveyed from one to another is to me so great an absurdity that I believe no man who has … any competent faculty of thinking can ever fall into it."[1]

Intrinsic energy is independent of mass and velocity. Intrinsic energy is the inherent energy of particles such as the proton and electron. Neutrons are composite particles composed of protons, electrons, and binding energy. Atoms, composed of protons, neutrons, and electrons, are the substance of larger three-dimensional physical entities, from molecules to galaxies.

Gravitation, electromagnetism, and other action at a distance phenomenon are mediated by gravitons, quantons and neutrinos. Gravitons, quantons and neutrinos are quanta that have a discrete amount of intrinsic energy and are emitted by particles in one direction at a time and absorbed by particles from one direction at a time. Emission-absorption events can be chirality meshing interactions that produce accelerations or achiral interactions that do not produce accelerations. Chirality meshing absorption of gravitons produces attractive accelerations, chirality meshing absorption of quantons produces either attractive or repulsive accelerations, and achiral absorption of neutrinos do not produce accelerations. The word neutrino is burdened with non-physical associations thus achiral quanta are henceforth called neutral flux.

A single chirality meshing interaction produces a deflection (a change in position), but a series of chirality meshing interactions produces acceleration (serial deflections). A single deflection in the direction of existing motion produces a small finite positive acceleration (and inertia) and a single deflection in the direction opposite existing motion produces a small finite negative acceleration (and inertia).

There are two fundamental differences between the mechanisms of Newtonian gravitation and discrete gravitation. The first is the Newtonian probability two particles will gravitationally interact is 100% but the discrete probability two particles will gravitationally interact is significantly less. The second difference is the treatment of force. In Newtonian physics a gravitational force between objects always exists, the force is infinitesimal and continuous, and ***the strength of the force*** is inversely proportional to the square of the separation distance. In discrete physics the existence of a gravitational force is dependent on the orientations of the particles of which objects are composed, the force is discrete and discontinuous, and ***the number of interactions*** is inversely proportional to the square of the separation distance. While there are considerable differences in mechanisms, in many phenomena the solutions of Newtonian and discrete gravitational equations are nearly identical.

[1] Original letter from Isaac Newton to Richard Bentley, 189.R.4.47, ff. 7-8, Trinity College Library, Cambridge, UK http://www.newtonproject.ox.ac.uk

There are similar fundamental differences between mechanisms of electromagnetic phenomena and in many cases the solutions of infinitesimal and discrete equations are nearly identical.

A particle emits gravitons and quantons at a rate proportional to particle intrinsic energy. A particle absorbs gravitons and quantons, subject to availability, at a maximum rate proportional to particle intrinsic energy. Each graviton or quanton emission event reduces the intrinsic energy of the particle and each graviton or quanton absorption event increases the intrinsic energy of the particle. Because graviton and quanton emission events continually occur but graviton and quanton absorption events are dependent on availability, these mechanisms collectively reduce the intrinsic energy of particles.

Only particles in nuclear reactions or undergoing radioactive disintegration emit neutral flux but in the solar system all particles absorb all available neutral flux.

In the solar system, discrete gravitational interactions mediate orbital phenomena and, for objects in a stable orbit the intrinsic energy loss due to the emission-absorption of gravitons is balanced by the absorption of intrinsic energy in the form of solar neutral flux.

Within the solar system, particle absorption of solar neutral flux (passing through a unit area of a spherical shell centered on the sun) adds intrinsic energy at a rate proportional to the inverse square of orbital distance, and over a relatively short period of time, the graviton, quanton, and neutral flux emission-absorption processes achieve Stable Balance resulting in constant intrinsic energy for particles of the same type at the same orbital distance, with particle intrinsic energies higher the closer to the sun and lower the further from the sun.

The process of Stable Balance is bidirectional.

If a high energy body consisting of high energy particles is captured by the solar gravitational field and enters into solar orbit at the orbital distance of earth, the higher particle intrinsic energies will result in an excess of intrinsic energy emissions compared to intrinsic energy absorptions at that orbital distance, and the intrinsic energy of the body will be reduced to bring it into Stable Balance.

If, on the other hand, a low energy body consisting of low energy particles is captured by the solar gravitational field and enters into solar orbit at the orbital distance of earth, the lower particle intrinsic energies will result in an excess of intrinsic energy absorptions at that orbital distance compared to the intrinsic energy emissions, and the intrinsic energy of the body will be increased to bring it into Stable Balance.

In an ideal two-body earth-sun system, a spherical and randomly symmetrical earth is in Stable Balance orbit about a spherical and randomly symmetrical sun. A randomly symmetrical body is composed of particles that collectively emit an equal intensity of gravitons (graviton flux) through a unit area on a spherical shell centered on the emitting body.

Unless otherwise stipulated, in this document references to the earth or sun assume they are part of an ideal two-body earth-sun system.

The gravitational intrinsic energy of earth is proportional to the gravitational intrinsic energy of the sun because total emissions of solar gravitons are proportional to the number of gravitons passing into or through earth as it continuously moves on a spherical shell centered on the sun (and also proportional to the volume of the spherical earth, to the cross-sectional area of the earth, to the diameter of the earth and to the radius of the earth).

Likewise, because the sun and the earth orbit about their mutual barycenter, the gravitational intrinsic energy of the sun is proportional to the gravitational intrinsic energy of the earth because total emissions of earthly gravitons are proportional to the number of gravitons passing into or through the sun as it continuously moves on a spherical shell centered on the earth (and also proportional to the volume of the spherical sun, to the cross-sectional area of the sun, to the diameter of the sun and to the radius of the sun).

We define the orbital distance of earth equal to 15E10 meters and note earth's orbit in an ideal two-body system is circular. If additional planets are introduced, earth's orbit will become elliptical and the diameter of earth's former circular orbit will be equal to the semi-major axis of the elliptical orbit.

$$d_{\oplus} = 15x10^{10} \ \left(\mathrm{m}\right)$$

We define the intrinsic photon velocity *c* equal to 3E8 m/s and equal in amplitude to the intrinsic constant *Theta* which is non-denominated. We further define the elapsed time for a photon to travel 15E10 meters equal to 500 seconds.

$$c = 3x10^{8} \ \left(\frac{\mathrm{m}}{\mathrm{s}}\right)$$
$$\theta = 3x10^{8} \ \left(\text{non-denominated}\right)$$
$$\frac{d_{\oplus}}{c} = 500 \ \left(\mathrm{s}\right)$$

The non-denominated intrinsic constant *Psi*, 1E-7, is equal in amplitude to the intrinsic magnetic constant denominated in units of Henry per meter.

$$\psi = 1x10^{-7} \ \left(\text{non-denominated}\right)$$
$$\mu_i = 1x10^{-7} \ \left(\frac{\mathrm{H}}{\mathrm{m}}\right)$$

Psi is also equal in amplitude to the 2014 CODATA vacuum magnetic permeability divided by 4π (after 2014 CODATA values for permittivity and permeability are defined and no longer reconciled to the speed of light); half the electromagnetic force (units of Newton) between two straight ideal (constant diameter and homogeneous composition) parallel conductors with center-to-center distance of one meter and each carrying a current of one Ampere; and to the intrinsic voltage of a magnetically induced minimum amplitude current loop (3E8 electrons per second).

The intrinsic electric constant, the inverse of the product of the intrinsic magnetic constant and the square of the intrinsic photon velocity, is equal to the inverse of 9E9 and denominated in units of Farad per meter.

$$\varepsilon_i = \frac{1}{\mu_i c^2} = \frac{1}{9x10^9} = 1.111111x10^{-10} \ \left(\frac{\mathrm{F}}{\mathrm{m}}\right)$$

The Newtonian mass of earth, denominated in units of kilogram, is equal to 6E24, and equal in amplitude to the active gravitational mass of earth, denominated in units of Einstein (the unit of intrinsic energy).

$$M_{\oplus N} = 6x10^{24} \ (\mathrm{kg}) \doteq M_{\oplus G} = 6x10^{24} \ (\mathrm{E})$$

The active gravitational mass is proportional to the number of gravitons emitted and the Newtonian mass is proportional to the number of gravitons absorbed. Every graviton absorbed contributes to the acceleration and inertia of the absorber, therefore the Newtonian mass is also the inertial mass.

We define the radius of earth, the square root of the ratio of the Newtonian inertial mass of earth divided by orbital distance, or the square root of the ratio of the active gravitational mass of earth divided by its orbital distance, equal to the square root of 4E13, 6.325E6, about 0.993 the NASA volumetric radius of 6.371E6. Our somewhat smaller earth has a slightly higher density and a local gravitational constant equal to 10 m/s2 at any point on its perfectly spherical surface.

$$r_\oplus = \sqrt{\frac{M_{\oplus N}}{d_\oplus}} = \sqrt{\frac{M_{\oplus G}}{d_\oplus}} = \sqrt{4x10^{13}} = 6.324555x10^6 \ (\mathrm{m})$$

$$g_\oplus = 10 \ \left(\frac{\mathrm{m}}{\mathrm{s}^2}\right)$$

We define the Gravitational constant at the orbital distance of earth, the ratio of the local gravitational constant of earth divided by its orbital distance, equal to the inverse of 15E9.

$$G_\oplus = \frac{g_\oplus}{d_\oplus} = \frac{10}{15x10^{10}} = \frac{1}{15x10^9} = 6.666666x10^{-11} \ \left(\frac{\mathrm{m}^3}{\mathrm{kg\ s}^2}\right)$$

The unit kilogram is equal to the mass of 6E26 protons at the orbital distance of earth, and the proton mass equal to the inverse of 6E26.

$$m_p = \frac{1}{6x10^{26}} = 1.666666x10^{-27} \ \ (\text{kg})$$

The proton intrinsic energy at the orbital distance of earth is equal to the inverse of the product of the proton mass and the mass-energy factor *delta* (equal to 100). Within the solar system, the proton intrinsic energy increases at orbital distances closer to the sun and decreases at orbital distances further from the sun. Changes in proton intrinsic energy are proportional to the inverse square of orbital distance.

$$E_p = \frac{1}{\delta m_p} = \frac{1}{6x10^{28}} = 1.666666x10^{-29} \ \ (\text{E})$$

$$\delta = \frac{m_p}{E_p} = 100$$

The Newtonian mass of the sun, denominated in units of kilogram, is equal to 2E30, and equal in amplitude to the active gravitational mass of the sun, denominated in units of Einstein.

$$M_{\odot N} = 2x10^{30} \ \ (\text{kg}) \ \doteq \ M_{\odot G(E)} = 2x10^{30} \ \ (\text{E})$$

The active gravitational mass is proportional to the number of gravitons emitted and the Newtonian mass is proportional to the number of gravitons absorbed. Every graviton absorbed contributes to the acceleration and inertia of the absorber, therefore the Newtonian mass is also the inertial mass.

The active gravitational mass of earth divided by the active gravitational mass of the sun is equal to the intrinsic constant *Beta-square* and its square root is equal to the intrinsic constant *Beta*.

$$\frac{M_{\oplus G(E)}}{M_{\odot G(E)}} = \beta^2 = 3x10^{-6}$$

$$\beta = 1.732050x10^{-3}$$

The charge intrinsic energy e_i, denominated in units of intrinsic Volt, is proportional to the number of quantons emitted by an electron or proton. The charge intrinsic energy is equal to *Beta* divided by *Theta-square*, the inverse of the square root of 27E38.

$$e_i = \frac{\beta}{\theta^2} = \frac{1}{\sqrt{27x10^{38}}} = 1.92450089x10^{-20} \ \ (\text{V}_\text{i})$$

Intrinsic voltage does not dissipate kinetic energy.

The electron intrinsic energy *Ee*, equal to the ratio of *Beta-square* divided by *Theta-cube*, the ratio of *Psi-square* divided by *Theta-square*, the product of the square of the charge intrinsic energy and *Theta*, and the ratio of the intrinsic electron magnetic flux quantum divided by the intrinsic Josephson constant, is denominated in units of Einstein.

$$E_{e(E)} = \frac{\beta^2}{\theta^3} = \frac{\psi^2}{\theta^2} = e_i^2\theta = \frac{\Phi_{0ei}}{K_{Ji}} = \frac{1}{9x10^{30}} \quad (\mathrm{E})$$

The intrinsic electron magnetic flux quantum, equal to the square root of the electron intrinsic energy, is denominated in units of intrinsic Volt second.

$$\Phi_{0ei} = \sqrt{E_e} = \frac{1}{3x10^{15}} = 3.333333x10^{-16} \quad (\mathrm{V_i s})$$

The intrinsic Josephson constant, equal to the inverse of the square root of the electron intrinsic energy, the ratio of *Theta* divided by *Psi* and the ratio of the photon velocity divided by the intrinsic sustaining voltage of a minimum amplitude superconducting current, is denominated in units of Hertz per intrinsic Volt.

$$K_{Ji} = \frac{1}{\sqrt{E_e}} = \frac{\theta}{\psi} = \frac{c}{V_{iS}} = 3x10^{15} \quad \left(\frac{\mathrm{Hz}}{\mathrm{V_i}}\right)$$

The discrete (dissipative kinetic) electron magnetic flux quantum, equal to the product of 2π and the intrinsic electron magnetic flux quantum, is denominated in units of discrete Volt second, and the discrete rotational Josephson constant, equal to the intrinsic Josephson constant divided by 2π and the inverse of the discrete electron magnetic flux quantum, is denominated in units of Hertz per discrete Volt. These constants are expressions of rotational frequencies.

$$\Phi_{0ed} = 2\pi\ \Phi_{0ei} = 2.094395x10^{-15} \quad (\mathrm{V_d s})$$

$$K_{Jdr} = \frac{K_{Ji}}{2\pi} = \frac{1}{\Phi_{0ed}} = 4.7746848x10^{14} \quad \left(\frac{\mathrm{Hz}}{\mathrm{V_d}}\right)$$

We define the electron amplitude equal to 1. The proton amplitude is equal to the ratio of the proton intrinsic energy divided by the electron intrinsic energy.

$$a_e = 1$$

$$a_p = \frac{E_p}{E_e} = \frac{\left(1/6x10^{28}\right)}{\left(1/9x10^{30}\right)} = 150$$

We define the Coulomb, $e_{c,}$ equal to the product of the charge intrinsic energy and the square root of the proton amplitude divided by two. The Coulomb denominates dissipative current.

$$e_c = e_i\sqrt{\frac{a_p}{2}} = \frac{1}{6x10^{18}} = 1.666666x10^{-19} \quad (\mathrm{C})$$

We define the Faraday equal to 1E5, and the Avogadro constant equal to the Faraday divided by the Coulomb.

$$\Im = 1x10^5 \left(\frac{\mathrm{C}}{\mathrm{mole}}\right)$$

$$N_A = \frac{\Im}{e_c} = 6x10^{23} \left(\frac{\mathrm{units}}{\mathrm{mole}}\right)$$

Lambda-bar, the quantum of particle intrinsic energy, equal to the intrinsic energy content of a graviton or quanton, is the ratio of the product of *Psi* and *Beta* divided by *Theta-cube*, the ratio of *Psi-cube* divided by the product of *Beta* and *Theta-square*, the product of the charge intrinsic energy and the intrinsic electron magnetic flux quantum, and the charge intrinsic energy divided by the intrinsic Josephson constant.

$$ƛ = \frac{\psi\beta}{\theta^3} = \frac{\psi^3}{\beta\theta^2} = e_i\Phi_{0ei} = \frac{e_i}{K_{Ji}} = \frac{1}{9\sqrt{3}x10^{34}} \quad (\mathrm{E})$$

CODATA physical constants that are defined as exact have an uncertainty of 10-12 decimal places therefore the exactness of Newtonian infinitesimal calculations is of a similar order of magnitude. We assert that *Lambda-bar* and proportional physical constants are discretely exact (equivalent to Newtonian infinitesimal calculations) because discretely exact physical properties can be exactly expressed to greater accuracy than can be measured in the laboratory.

All intrinsic physical constants and intrinsic properties are discretely rational. The ratio of two positive integers is a discretely rational number.

- The ratio of two discretely rational numbers is discretely rational.
- The rational power or rational root of a discretely rational number is discretely rational.
- The difference or sum of discretely rational numbers is discretely rational. This property is important in the derivation of atomic spectra where it serves the same purpose as a Fourier transform in infinitesimal mathematics.

The intrinsic electron gyromagnetic ratio, equal to the ratio of the cube of the charge intrinsic energy divided by *Lambda-bar* square, is denominated in units of Hertz per Tesla.

$$\gamma_e = \frac{e_i^3}{ƛ^2} = \sqrt{3x10^{22}} = 1.732050x10^{11} \left(\frac{\mathrm{Hz}}{\mathrm{T}}\right)$$

The intrinsic proton gyromagnetic ratio, equal to the ratio the intrinsic electron gyromagnetic ratio divided by the square root of the cube of the proton amplitude divided by two and the ratio of eight times the photon velocity divided by nine, is denominated in units of Hertz per Tesla.

$$\gamma_p = \frac{\gamma_e}{\sqrt{\left(a_p \diagup 2\right)^3}} = \frac{8c}{9} = 2.666666x10^8 \ \left(\frac{\mathrm{Hz}}{\mathrm{T}}\right)$$

The intrinsic conductance quantum, equal to the product of the intrinsic Josephson constant and the discrete Coulomb, is denominated in units of intrinsic Siemen.

$$G_{0i} = K_{Ji} e_c = 5x10^{-4} \ \left(\mathrm{S_i}\right)$$

The kinetic conductance quantum, equal to the intrinsic conductance quantum divided by 2π, is denominated in units of kinetic Siemen.

$$G_{0k} = \frac{G_{0i}}{2\pi} = 7.957747x10^{-5} \ \left(\mathrm{S_k}\right)$$

The CODATA conductance quantum is equal to 7.748091E-5.

The intrinsic resistance quantum, equal to the inverse of the intrinsic conductance quantum, is denominated in units of Ohm.

$$R_{0i} = \frac{1}{G_{0i}} = 2000 \ \left(\Omega\right)$$

The kinetic resistance quantum, equal to the inverse of the kinetic conductance quantum, is denominated in units of Ohm.

$$R_{0k} = \frac{1}{G_{0k}} = 1.256637x10^4 \ \left(\Omega\right)$$

The CODATA resistance quantum is equal to 1.290640E4.

The intrinsic von Klitzing constant, equal to the ratio of the discrete Planck constant divided by the square of the intrinsic electric constant, is denominated in units of Ohm.

$$R_{Ki} = \frac{h}{e_i^2} = 1.800000x10^6 \ \left(\Omega\right)$$

The kinetic von Klitzing constant, equal to the ratio of the discrete Planck constant divided by the square of the discrete Coulomb, is denominated in units of Ohm.

$$R_{Kk} = \frac{h}{e_c^2} = 2.592000x10^4 \ \ (\Omega)$$

The CODATA von Klitzing constant is equal to 2.581280745E4.

In Newtonian physics the probability particles at a distance will interact is 100% but in discrete physics a certain granularity is needed for interactions to occur.

A particle G-axis is a single-ended hollow cylinder. The mechanism of the G-axis is analogous to a piston which moves up and down at a frequency proportional to particle intrinsic energy. At the end of the up-stroke a single graviton is emitted and during a down-stroke the absorption window is open until the end of the downstroke or the absorption of a single graviton.

The difference (the intrinsic granularity) between the inside diameter of the hollow cylindrical G-axis and the outside diameter of the graviton allows absorption of incoming gravitons at angles that can deviate from normal (straight down the center) by plus or minus 20 arcseconds.

There are three kinds of intrinsic granularity: the intrinsic granularity in phenomena mediated by the absorption of gravitons and quantons; the intrinsic granularity in phenomena mediated by the emission of gravitons and quantons; and the intrinsic granularity in certain electromagnetic phenomena.

- The intrinsic granularity in phenomena mediated by the absorption of gravitons or quantons by particles in tangible objects (with kilogram mass greater than one microgram or 1E20 particles) is discretely infinite therefore the average value of 20 arcseconds is discretely exact.
- The intrinsic granularity in phenomena mediated by the emission of gravitons or quantons by particles is 20 arcseconds because gravitons and quantons emitted in the direction in which the emitting axis is pointing have an intrinsic granularity of not more than plus or minus 10 arcseconds.
- The intrinsic granularity of certain electromagnetic phenomena, in particular a Faraday disk generator, governed by a “Lorentz force” that causes the velocity of an electron to be at a right angle to the force also causes an additional directional change of 20 arcseconds in the azimuthal direction.

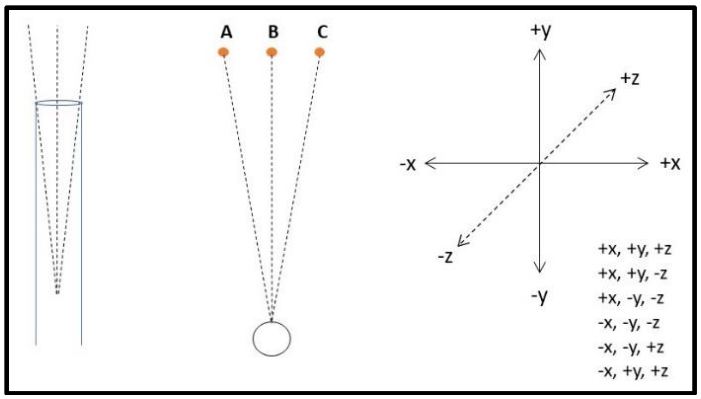

In the above diagram, the intrinsic granularity of graviton absorption is illustrated on the left.

Above center illustrates the aberration between the visible and the actual positions of the sun with respect to an observer on earth as the sun moves across the sky. Position A is the visible position of the sun, position B is the actual position of the sun, position B will be the visible position of the sun in 500 seconds, and position C will be the actual position of the sun in 500 seconds. The elapsed time between successive positions is proportional to the separation distance, but 20 arcseconds of aberration is independent of separation distance.

Above right illustrates the six directions within a Cartesian space and the six possible forms describing the six possible facing directions in which a vector can point. A vector pointing up the G-axis of particle A in the facing direction of particle B has one and only one of the six possible forms. The probability a gravitational interaction will occur, if the vector is facing in one of the other five facing directions, is zero. Therefore, a gravitational interaction involving a graviton emitted by a specific particle A and absorbed by a specific particle B is possible (not probable) in only one-sixth the total volume of Cartesian space.

We define the intrinsic steric factor equal to 6. The intrinsic steric factor is inversely proportional to the probability a specific gravitational intrinsic energy interaction ***can*** occur on a scale where the probability a Newtonian gravitational interaction ***will*** occur is 100%.

$$S_{\varnothing i} = 6$$

The intrinsic steric factor points outward from a specific particle located at the origin of a Cartesian space facing outward into the surrounding space. The intrinsic steric factor applies to action at a distance in phenomena mediated by gravitons and quantons.

To convert 20 arcseconds of intrinsic granularity into an inverse possibility, divide the 1,296,000 arcseconds in 360 degrees by the product of 20 arcseconds and the intrinsic steric factor.

$$\frac{1,296,000}{20S_{\varnothing i}} = 10,800$$

A possibility is not the same as a probability. The possibility two particles ***can*** gravitationally interact (each with the other) is equal to 1 out of 10,800. The probability two particles ***will*** gravitationally interact (each with the other) is dependent on the geometry of the interaction.

Because Newtonian gravitational interactions are proportional to the quantum of kinetic energy, the discrete Planck constant, and discrete gravitational interactions are proportional to the quantum of intrinsic energy, *Lambda-bar,* the factor 10,800 is a conversion factor.

In a bidirectional gravitational interaction, the ratio of the square of the discrete Planck constant divided by the square of *Lambda-bar* is equal to 10,800.

In a one-directional gravitational interaction the ratio of the discrete Planck constant divided by *Lambda-bar* is equal to the square root of 10,800.

The discrete Planck constant is equal to *Lambda-bar* times the square root of 10,800 and denominated in units of Joule second.

$$h = \lambda\!\!\!^{-}\sqrt{10800} = \frac{1}{15x10^{32}} = 6.666666x10^{-34} \quad (\mathrm{Js})$$

The value of the discrete Planck constant, approximately 1.006 times larger than the 2018 CODATA value, is the correct value for the two-body earth-sun system and proportional to the intrinsic physical constants previously defined.

The CODATA fine structure constant *alpha* is equal to the ratio of the square of the CODATA electron charge divided by the product of two times the CODATA Planck constant, the CODATA vacuum permittivity and the CODATA speed of light (2018 CODATA values).

The intrinsic constant *Beta* is a transformation of the CODATA expression.

By substitution of the charge intrinsic energy for the CODATA electron charge, *Lambda-bar* for two times the CODATA Planck constant, the intrinsic electric constant for the CODATA vacuum permittivity and the intrinsic photon velocity for the CODATA speed of light, the dimensionless CODATA fine structure constant *alpha* is transformed into the dimensionless intrinsic constant *Beta.*

$$\alpha = \frac{e^2}{2h\varepsilon_0 c} = 7.2973525693x10^{-3} \quad \rightarrow \quad \beta = \frac{e_i^2}{\lambda\!\!\!^{-}\varepsilon_i c} = \sqrt{3}x10^{-3} = 1.732050x10^{-3}$$

The existence of the fine structure constant and its ubiquitous appearance in seemingly unrelated equations is due to the assumption that phenomena are governed by kinetic energy, consequently measured values of phenomena governed or partly governed by intrinsic energy do not agree with the theoretical expectations.

A gravitational phenomenon governed by intrinsic energy is the solar system Kepler constant equal to the square root of the cube of the planet's orbital distance divided by 4π-square times the orbital period of the planet, the product of the active gravitational mass of the sun and the Gravitational constant at the orbital distance of earth divided by 4π-square, and the ratio of the product of the square of the planet's velocity and the orbital distance of the planet divided by 4π-square.

$$K_p = \frac{\sqrt{d_p^3}}{4\pi^2 P_p} = \frac{M_{\odot G(E)} G_{\oplus}}{4\pi^2} = \frac{v_p^2 d_p}{4\pi^2}$$

The intrinsic constant *Beta-square*, previously shown to be the ratio of the active gravitational mass of earth divided by the active gravitational mass of the sun, is also proportional to the key orbital properties of the sun, earth, and moon.

$$\frac{M_{\oplus G(E)}}{M_{\odot G(E)}} = B^2 = \sqrt{\frac{v_{\oplus}^2 d_{\oplus}}{v_{\odot}^2 d_{\odot}}} = \sqrt{\frac{K_{\oplus}}{K_{\odot}}} = \frac{v_m^2 d_m}{v_{\oplus}^2 d_{\oplus}} = \frac{K_m}{K_{\oplus}}$$

An electromagnetic phenomenon governed by intrinsic energy is the proton-electron mass ratio, here termed the electron-proton deflection ratio, equal to the square root of the cube of the proton intrinsic energy divided by the cube of the electron intrinsic energy, and to the square root of the cube of the proton amplitude divided by the cube of the unit electron amplitude.

$$\text{electron-proton deflection ratio} = \sqrt{\frac{E_p^3}{E_e^3}} = \sqrt{\frac{a_p^3}{a_e^3}} = \sqrt{\frac{150^3}{1^3}} = 1837.11730708$$

The CODATA proton-electron mass ratio is a measure of electron deflection (1836.15267344) in units of proton deflection (equal to 1). Because the directions of proton and electron deflections are opposite, the electron-proton deflection ratio is approximately equal to the CODATA proton-electron mass ratio plus one.

$$\text{electron-proton deflection ratio} \approx 1836.15267344 + 1 = 1837.15267344$$

$$\frac{(\text{CODATA proton-electron mass ratio}) + 1}{\text{electron-proton deflection ratio}} = \frac{1837.15267344}{1837.11730708} = 1.00001925$$

In this document, unless otherwise specified (as in CODATA constants denominated in units of Joule proportional to the CODATA Planck constant), units of Joule are proportional to the discrete Planck constant.

The ratio of the discrete Planck constant divided by *Lambda-bar*, equal to the product of the mass-energy factor *delta* and *omega-2*, is denominated in units of discrete Joule per Einstein.

$$\frac{h}{\lambda\!\!\!^{-}} = \sqrt{10800} = \delta\omega^2 = 103.9230 \left(\frac{\mathrm{J_d}}{\mathrm{E}}\right)$$

In the above equation the denomination discrete Joule represents energy proportional to the discrete Planck constant and the denomination Einstein represents energy proportional to *Lambda-bar*. The mass-energy factor *delta* converts non-collisional energy (action at a distance) into collisional energy in units of intrinsic Joule. The factor *omega-2* converts units of intrinsic Joule into units of discrete Joule.

Omega factors correspond to the geometry of graviton-mediated and quanton-mediated phenomena.

We will begin with a brief discussion of electrical (quanton-mediated) phenomena then exclusively focus on gravitational phenomena for the remainder of Part One.

Electrical phenomena

The discrete steric factor, equal to 8, is the number of octants defined by the orthogonal planes of a Cartesian space.

$$S_{\varnothing d} = 8$$

Each octant is one of eight signed triplets (---, -+-, -++, --+, +++, +-+, +--, ++-) which correspond to the direction of the x, y, and z Cartesian axes.

A large number of random molecules, each with a velocity coincident with its center of mass, are within a Cartesian space. If the origin is the center of mass of specific molecule1, then random molecule2 is within one of the eight signed octants and, because the same number of random molecules are within each octant, then the specific molecule1 is within one of the eight signed octants with respect to random molecule2, and the possibility (not probability) of a center of mass collisional interaction between molecule2 and molecule1 is equal to the inverse of the discrete steric factor (one in eight).

The discrete and intrinsic steric factors correspond to the geometries of phenomena governed by discrete kinetic energy (proportional to the discrete Planck constant) and to phenomena governed by intrinsic energy:

- The discrete steric factor points inward from a random molecule in the direction of a specific molecule and applies to phenomena mediated by collisional interactions.
- The intrinsic steric factor points outward from a specific particle into the surrounding space and applies to phenomena mediated by gravitons and quantons (action at a distance).

The intrinsic molar gas constant, equal to the discrete steric factor, is the intrinsic energy (units of intrinsic Joule) divided by mole Kelvin.

$$R_i = S_{\varnothing d} = 8 \left(\frac{\mathrm{J_i}}{\mathrm{mol} \cdot \mathrm{K}} \right)$$

The discrete molar gas constant, equal to the product of the intrinsic molar gas constant and *omega-2*, is the intrinsic energy (units of discrete Joule) divided by mole Kelvin. The discrete molar gas constant agrees with the CODATA value within 1 part in 13,000.

$$R_d = R_i \omega^2 = \frac{24\sqrt{3}}{5} = 8.3138438 \left(\frac{\mathrm{J_d}}{\mathrm{mol} \cdot \mathrm{K}} \right)$$

The ratio of the CODATA electron charge (the elementary charge in units of Coulomb) divided by the charge intrinsic energy (in units of intrinsic Volt) is nearly equal to the discrete molar gas constant.

$$\frac{e \ \mathrm{CODATA}}{e_i} = 8.325153$$

$$\frac{8.325153}{R_d} = \frac{8.325153}{8.313843} = 1.001360$$

The intrinsic Boltzmann constant, equal to the ratio of the intrinsic molar gas constant divided by the Avogadro constant, is denominated in units of Einstein per Kelvin.

$$k_i = \frac{R_i}{N_A} = \frac{1}{75x10^{21}} = 1.333333x10^{-23} \left(\frac{\mathrm{E}}{\mathrm{K}} \right)$$

The discrete Boltzmann constant, equal to the product of *omega-2* and the intrinsic Boltzmann constant, and the ratio of the discrete molar gas constant divided by the Avogadro constant, is denominated in units of discrete Joule per Kelvin. The CODATA Boltzmann constant is equal to 1.380649×10^{-23}.

$$k_d = \omega^2 k_i = \frac{R_d}{N_A} = 1.385640 x 10^{-23} \left(\frac{\mathrm{J}_{\mathrm{d}}}{\mathrm{K}} \right)$$

Gravitational phenomena

Omega-2, the square root of 1.08, corresponds to one-directional gravitational interactions between non-orbiting objects (objects not by themselves in orbit, that is, the object might be part of an orbiting body but the object itself is not the orbiting body), for example graviton emission by the large lead balls or absorption by the small lead balls in the Cavendish experiment.

$$\omega^2 = \sqrt{\frac{h}{\delta \lambda\!\!\!^{-}}} = \sqrt{1.08} = 1.039230$$

Omega-4, 1.08, corresponds to two-directional gravitational interactions (emission and absorption) between non-orbiting objects, for example the acceleration of the large lead balls *or* the acceleration of the small lead balls in the Cavendish experiment.

$$\omega^4 = \frac{h}{\delta \lambda\!\!\!^{-}} = 1.08$$

Omega-6, the square root of the cube of 1.08, corresponds to gravitational interactions between a planet and moon in a Keplerian orbit where the square root of the cube of the orbital distance divided by the orbital period is equal to a constant.

$$\omega^6 = \sqrt{\frac{h^3}{\delta^3 \lambda\!\!\!^{-3}}} = \sqrt{(1.08)^3} = 1.122368$$

Omega-8, the square of 1.08, corresponds to four-directional gravitational interactions by non-orbiting objects, for example the acceleration of the small lead balls *and* the acceleration of the large lead balls in the Cavendish experiment.

$$\omega^8 = \frac{h^2}{\delta^2 \lambda\!\!\!^{-2}} = 1.08^2 = 1.166400$$

Omega-12, equal to the cube of 1.08, corresponds to gravitational interactions between two objects in orbit about each other, for example the sun and a planet in orbit about their mutual barycenter.

$$\omega^{12} = \frac{h^3}{\delta^3 \lambda^3} = 1.08^3 = 1.259712$$

Except where previously defined (the Gravitational constant at the orbital distance of earth, the orbital distance of earth, the mass and volumetric radius of earth, the mass of the sun) the following equations use the NASA[2] values for the Newtonian masses, orbital distances, and volumetric radii of the planets.

The local gravitational constant for any of the planets is equal to the product of the Gravitational constant of earth and the Newtonian mass (kilogram mass) of the planet divided by the square of the volumetric radius of the planet.

$$g_p = \frac{G_\oplus M_{pN}}{r_p^2} = 10(\text{earth}) = 25.89069(\text{jupiter}) \ \ (\text{Newtonian})$$

The v2d value of a planetary moon is equal to the product of the Gravitational constant at the orbital distance of earth and the Newtonian mass of the planet.

$$(v^2 d)_{\text{moon}} = G_\oplus M_{pN} = 4.0000x10^{14}(\text{earth}) = 1.265420x10^{17}(\text{jupiter}) \ \ (\text{Newtonian})$$

The active gravitational mass of a planet, denominated in units of Einstein, is equal to the product of the square of the volumetric radius of the planet and the orbital distance of the planet, divided by the square of the orbital distance of the planet in units of the orbital distance of earth.

$$M_{pG(E)} = \frac{r_p^2 d_p}{(d_p / d_\oplus)^2} = 6x10^{24}(\text{earth}) = 1.412624x10^{26}(\text{jupiter}) \ \ (\text{E}) \ \ (\text{non-Newtonian})$$

The mass of a planet in a Newtonian orbit about the sun (the planet and sun orbit about their mutual barycenter) is a kinetic property. The active gravitational mass of such a planet, denominated in units of Joule, is equal to the product of the active gravitational mass of the planet in units of Einstein and *omega-12*.

$$M_{pG(J)} = M_{pG(E)} \ \omega^{12} = 7.558272x10^{24}(\text{earth}) = 1.779499x10^{26}(\text{jupiter}) \ \ (\text{J}) \ \ (\text{non-Newtonian})$$

[2] https://nssdc.gsfc.nasa.gov/planetary/planetfact.html, accessed Dec 24, 2021

The Gravitational constant at the orbital distance of the planet is equal to the product of the local gravitational constant of the planet and the square of the volumetric radius of the planet, divided by the active gravitational mass of the planet.

$$G_p = \frac{g_p r_p^2}{M_{pG(E)}} = 6.666666x10^{-11}\,(\text{earth}) = 8.957937x10^{-10}\,(\text{jupiter})\ \ (\text{non-Newtonian})$$

The v2d value of a planetary moon is equal to the product of the Gravitational constant at the orbital distance of the planet and the active gravitational mass of the planet.

$$\left(v^2 d\right)_{\text{moon}} = G_p M_{pG(E)} = 4.0000x10^{14}\,(\text{earth}) = 1.265420x10^{17}\,(\text{jupiter})\ \ (\text{non-Newtonian})$$

The v2d values calculated using the NASA orbital parameters for the moon is larger than the above calculated values by 1.00374; the v2d calculations using the NASA orbital parameters for the major Jovian moons (Io, Europa, Ganymede and Callisto) are larger than the above calculated values by 1.0020, 1.0016, 1.00131, and 1.00133.

Newtonian gravitational calculations are extremely accurate for most gravitational phenomena but there are a number of anomalies for which the Newtonian calculations are inaccurate. The first of these anomalies to come to the attention of scientists in 1859 was the precession rate of the perihelion of mercury for which the observed rate was about 43 arcseconds per century larger than the Newtonian calculated rate.[3]

According to Gerald Clemence, one of the twentieth century's leading authorities on the subject of planetary orbital calculations, the most accurate method for calculating planetary orbits, the method of Gauss, was derived for calculating planetary orbits within the solar system with distance expressed in astronomical units, orbital period in days and mass in solar masses.[4]

The Gaussian method was used by Eric Doolittle in what Clemence believed to be the most reliable theoretical calculation of the perihelion precession rate of mercury.[5]

With modifications by Clemence including newer values for planetary masses, newer measurements of the precession of the equinoxes and a careful analysis of the error terms, the calculated rate was determined to be 531.534 arc-seconds per century compared to the observed rate of 574.095 arc-seconds per century, leaving an unaccounted deficit of 42.561 arcseconds per century.

[3] Urbain Le Verrier, Reports to the Academy of Sciences (Paris), Vol 49 (1859)

[4] Clemence G.M. The relativity effect in planetary motions. Reviews of Modern Physics, 1947, 19(4): 361-364.

[5] Eric Doolittle, The secular variations of the elements of the orbits of the four inner planets computed for the epoch 1850 GMT, Trans. Am. Phil. Soc. 22, 37(1925).

The below calculations are based on the method of Price and Rush.[6] This method determines a Newtonian rate of precession due to the gravitational influences on mercury by the sun and five outer planets external to the orbit of mercury (venus, earth, mars, jupiter and saturn) The solar and planetary masses are treated as Newtonian objects and in calculations of planetary gravitational influences the outer planets are treated as circular mass rings.

The Newtonian gravitational force on mercury due to the mass of the sun is equal to ratio of the product of the negative Gravitational constant at the orbital distance of earth, the mass of the sun and the mass of mercury divided by the square of the orbital distance of mercury.

$$F_{\odot\to Merc} = \frac{-G_{\oplus} M_{\odot} M_{merc}}{d_{merc}^2} = -1.306377x10^{22} \quad (\mathrm{N}) \ (\mathrm{Newtonian})$$

The Newtonian gravitational force on mercury due to the mass of the five outer planets is equal to the sum of the gravitational force contributions of the five outer planets external to the orbit of mercury. The gravitational force contribution of each planet is equal to the ratio of the product of the Gravitational constant at the orbital distance of earth, the mass of the planet, the mass of mercury and the orbital distance of mercury, divided by the ratio of the product of twice the planet's orbital distance and the difference between the square of the planet's orbital distance and the square of the orbital distance of mercury.

$$F_{P's\to merc} = \sum_{p1-p5} \frac{G_{\oplus} M_{P1} M_{merc} d_{merc}}{2d_{P1}\left(d_{P1}^2 - d_{merc}^2\right)} = 7.513045x10^{15} \quad (\mathrm{N}) \ (\mathrm{Newtonian})$$

The gravitational force ratio is equal to the gravitational force on mercury due to the mass of the five outer planets external to the orbit of mercury divided by the gravitational force on mercury due to the mass of the sun.

$$F_{GF} = \frac{F_{P's\to merc}}{F_{\odot\to merc}} = -5.751054x10^{-7} \ (\mathrm{Newtonian})$$

The gamma factor is equal to the sum of the gamma contributions of the five outer planets external to the orbit of mercury. The gamma contribution of each planet is equal to the ratio of the product of the mass of the planet, the orbital distance of mercury, and the sum of the square of the planet's orbital distance and the square of the orbital distance of mercury, divided by the product of 2π, the planet's orbital distance and the square of the difference between the square of the planet's orbital distance and the square of the orbital distance of mercury.

$$\Gamma = \sum_{p1-p5} \frac{\left[M_{p1} d_{merc}\left(d_{p1}^2 + d_{merc}^2\right)\right]}{\left[2\pi d_{p1}\left(d_{p1}^2 - d_{merc}^2\right)^2\right]} = 155.684739 \ (\mathrm{Newtonian})$$

[6] Michael P. Price and William F. Rush, Nonrelativistic contribution to mercury's perihelion precession. Am. J. Phys. 47(6), June 1979.

Psi-mercury is equal to the product of π and the sum of one plus the difference between the negative of the gravitational force ratio and the ratio of the product of the Gravitational constant at the orbital distance of earth, π, the mass of mercury and the gamma factor divided by twice the gravitational force on mercury due to the mass of the sun.

$$\psi_{merc} = \pi\left(1+\left[-F_{GF}-\left(\frac{G_{\oplus}\pi M_{merc}\Gamma}{2F_{\odot\rightarrow merc}}\right)\right]\right) = 3.1415956132 \ \left(\text{Newtonian}\right)$$

The number of arc-seconds in one revolution is equal to 360 degrees times sixty minutes times sixty seconds.

$$A_{360} = 360x60x60 = 1,296,000$$

The number of days in a Julian century is equal to 100 times the length of a Julian year in days.

$$J_{c(d)} = 100x365.25 = 36,525$$

The perihelion precession rate of mercury is equal to the ratio of the product of the difference between 2ψ-mercury and 2π, the number of arc-seconds in one revolution and the number of days in a Julian century, divided by the product of 2π and the NASA sidereal orbital period of mercury in units of day (87.969).

$$\dot{\omega} = \frac{\left(2\psi_{merc}-2\pi\right)A_{360}J_{c(d)}}{2\pi P_{merc(d)}} = 531.395 \quad \left(\frac{\text{arcsec}}{\text{century}}\right) \ \left(\text{Newtonian}\right)$$

The Newtonian perihelion precession rate of mercury determined above is 0.139 arc-seconds per century less than the Clemence ***calculated*** rate of 531.534 arc-seconds per century.

The following equations, the same format as the Newtonian equations, derive the non-Newtonian values (when different).

The Newtonian gravitational force on mercury due to the mass of the sun is equal to ratio of the product of the negative Gravitational constant at the orbital distance of earth, the mass of the sun and the mass of mercury divided by the square of the orbital distance of mercury.

$$F_{\odot\rightarrow Merc} = \frac{-G_{\oplus}M_{\odot}M_{merc}}{d_{merc}^2} = -1.306377x10^{22} \quad \left(\text{N}\right) \ \left(\text{Newtonian}\right)$$

The non-Newtonian gravitational force on mercury due to the mass of the five outer planets is equal to the sum of the gravitational force contributions of the five outer planets external to the orbit of mercury. The gravitational force contribution of each planet is equal to the product of the ratio of the product of the Gravitational constant at the orbital distance of earth, the active gravitational mass (in units of Joule) of the planet, the Newtonian mass of mercury and the orbital distance of mercury, divided by the ratio of the product of twice the planet's orbital distance and the difference between the square of the planet's orbital distance and the square of the orbital distance of mercury.

$$F_{P's\rightarrow merc} = \sum_{p1-p5}\left(\frac{G_{\oplus}M_{pG(J)}M_{merc}d_{merc}}{2d_{P1}\left(d_{P1}^{2}-d_{merc}^{2}\right)}\right) = 8.852929x10^{15} \quad (\mathrm{N})\ (\text{non-Newtonian})$$

The non-Newtonian gravitational force ratio is equal to the gravitational force on mercury due to the mass of the five outer planets external to the orbit of mercury divided by the gravitational force on mercury due to the mass of the sun.

$$F_{GF} = \frac{F_{P's\rightarrow merc}}{F_{\odot\rightarrow merc}} = -6.6862572749x10^{-7}\ (\text{non-Newtonian})$$

The gamma factor is equal to the sum of the gamma contributions of the five outer planets external to the orbit of mercury. The gamma contribution of each planet is equal to the ratio of the product of the mass of the planet, the orbital distance of mercury, and the sum of the square of the planet's orbital distance and the square of the orbital distance of mercury, divided by the product of 2π, the planet's orbital distance and the square of the difference between the square of the planet's orbital distance and the square of the orbital distance of mercury.

$$\Gamma = \sum_{p1-p5}\frac{\left[M_{p1}d_{merc}\left(d_{p1}^{2}+d_{merc}^{2}\right)\right]}{\left[2\pi d_{p1}\left(d_{p1}^{2}-d_{merc}^{2}\right)^{2}\right]} = 155.684739\ (\text{Newtonian})$$

The non-Newtonian value for *Psi*-mercury is equal to the product of π and the sum of one plus the difference between the negative of the gravitational force ratio and the ratio of the product of the Gravitational constant at the orbital distance of earth, π, the mass of mercury and the gamma factor divided by twice the gravitational force on mercury due to the mass of the sun.

$$\psi_{Merc} = \pi\left(1+\left[-F_{GF}-\left(\frac{G_{\oplus}\pi M_{merc}\Gamma}{2F_{\odot\rightarrow merc}}\right)\right]\right) = 3.1415960470\ (\text{non-Newtonian})$$

The non-Newtonian perihelion precession rate of mercury is equal to the ratio of the product of the difference between 2ψ-mercury and 2π, the number of arc-seconds in one revolution and the number of days in a Julian century, divided by the product of 2π and the NASA sidereal orbital period of mercury in units of day (87.969).

$$\dot{\omega} = \frac{\left(2\psi_{merc} - 2\pi\right) A_{360} J_{c(d)}}{2\pi P_{merc(d)}} = 580.223 \quad \left(\frac{\text{arcsec}}{\text{century}}\right) \left(\text{non-Newtonian}\right)$$

The non-Newtonian perihelion precession rate of mercury is 6.128 arc-seconds per century greater than the Clemence ***observed*** rate of 574.095 arc-seconds per century.

We have built a model of gravitation proportional to the dimensions of the earth-sun system. A different model, with different values for the physical constants, would be equally valid if it were proportional to the dimensions of a different planet in our solar system or a planet in some other star system in our galaxy.

Our sun and the stars in our galaxy, in addition to graviton flux, emit large quantities of neutral flux that establish Stable Balance orbits for planets that emit relatively small quantities of neutral flux.

Our galactic center emits huge quantities of gravitons and neutral flux, and its dimensional relationship with our sun is dependent on the neutral flux emissions of our sun. If the intrinsic energy of our sun was less, its orbit would be further out from the galactic center, and if it was greater, its orbit would be closer in.

- Of two stars at the same distance from the galactic center with different velocities, the star with higher velocity has a higher graviton absorption rate (higher stellar internal energy) and the star with lower velocity has a lower graviton absorption rate (lower stellar internal energy).
- Of two stars with the same velocity at different distances from the galactic center, the star closer in will have a higher graviton absorption rate (higher stellar internal energy) and the star further out will have a lower graviton absorption rate (lower stellar internal energy).

The active gravitational mass of the Galactic Center is equal to the active gravitational mass of the sun divided by *Beta-fourth* and the cube of the active gravitational mass of the sun divided by the square of the active gravitational mass of earth.

$$\bar{M}_{\otimes G(E)} = \frac{\bar{M}_{\odot G(E)}}{\beta^4} = \frac{\bar{M}^3_{\odot G(E)}}{\bar{M}^2_{\oplus G(E)}} = \frac{2x10^{42}}{9} = 2.222222x10^{41}$$

The second expression of the above equation, generalized and reformatted, asserts the square root of the cube of the active gravitational mass of any star in the Milky Way divided by the active gravitational mass of any planet in orbit about the star is equal to a constant.

$$\frac{\sqrt{M^{3}_{StarG(E)}}}{M_{PlanetG(E)}} = \text{constant}$$

The above equation, combined with the detailed explanation of the chirality meshing interactions that mediate gravitational action at a distance, the derivation of solar system non-Newtonian orbital parameters, the derivation of the non-Newtonian rate of precession of the perihelion of mercury, and the detailed explanation of non-Newtonian stellar rotation curves, disproves the theory of dark matter.

Part Two

Structure and chirality

A particle has the property of chirality because its axes are orthogonal and directed, pointing in three perpendicular directions and, like the fingers of a human hand, the directed axes are either left-handed (LH) or right-handed (RH). The electron and antiproton exhibit LH structural chirality and the proton and positron exhibit RH structural chirality. The two chiralities are mirror images.

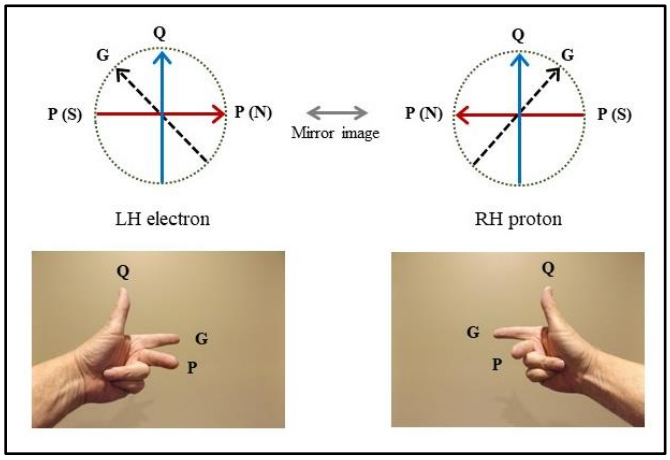

The electron G-axis (black, index finger) points into the paper, the electron Q-axis (blue, thumb) points up in the plane of the paper, and the north pole of the electron P-axis (red, middle finger) points right in the plane of the paper.

The orientation of the axes of an RH proton are the mirror image: the proton G-axis (black, index finger) points into the paper, the proton Q-axis (blue, thumb) points up in the plane of the paper, and the north pole of the proton P-axis (red, middle finger) points left in the plane of the paper.

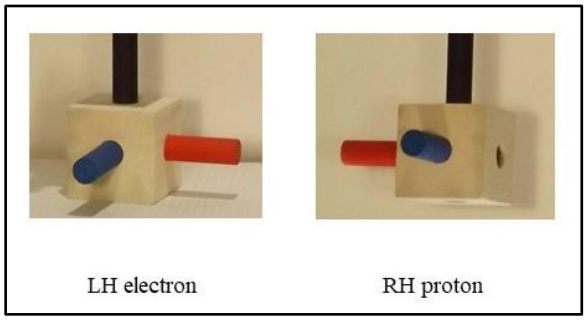

Above, to visualize orientations, models are easier to manipulate than human hands.

When Michael Faraday invented the disk generator in 1831, he discovered the conversion of rotational force, in the presence of a magnetic field, into electric current. The apparatus creates a magnetic field perpendicular to a hand-cranked rotating conductive disk and, providing the circuit is completed through a path external to the disk, produces an electric current flowing inward from axle to rim (electron flow not conventional current), photograph below.[7]

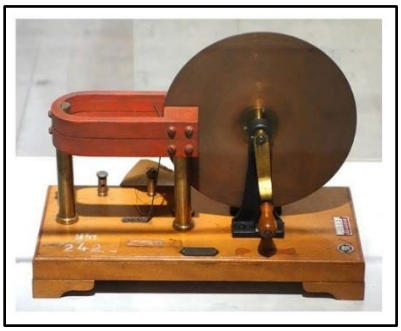

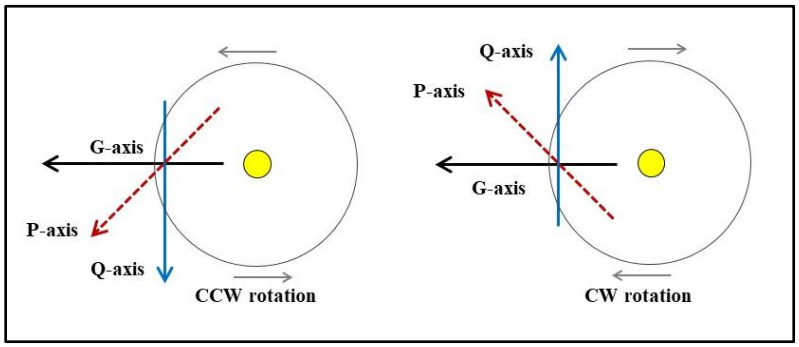

Above left, the electron Q-axis points in the CCW direction of motion. The inertial force within a rotating conductive disk aligns conduction electron G-axes to point in the direction of the rim. The alignment of the Q-axes and G-axes causes the orthogonal P-axes to point down.

Above right, the electron Q-axis points in the CW direction of motion. The inertial force within a rotating conductive disk aligns conduction electron G-axes to point in the direction of the rim. The alignment of the Q-axes and G-axes causes the orthogonal P-axes to point up.

In generally accepted physics (GAP), the transverse alignment of electron velocity with respect to magnetic field direction is attributed to the Lorentz force but, as explained above it is a consequence of electron chirality.

In addition to the transverse alignment of the electron direction with respect to the direction of the magnetic field, the electron experiences an additional directional change of 20 arcseconds in the azimuthal direction which causes the electron to spiral in the direction of the axle. Thus, in both a CCW rotating conductive disk and a CW rotating conductive disk, the current (electron flow not conventional current) flows from the axle to the rim.

[7] Wikimedia, by Daderot made available under the Creative Commons CC0 1.0 Universal Public Domain Dedication, location National Museum of Nature and Science, Tokyo, Japan.

The geometries of the Faraday disk generator apply to the orientation of conduction electrons in the windings of solenoids and transformers. CCW and CW windings advance in the same direction, below into the plane of the paper. In contrast to the rotating conductor in the disk generator, the windings are stationary, and the conduction electrons spiral through in the direction of the positive voltage supply (which continually reverses in transformers and AC solenoids).

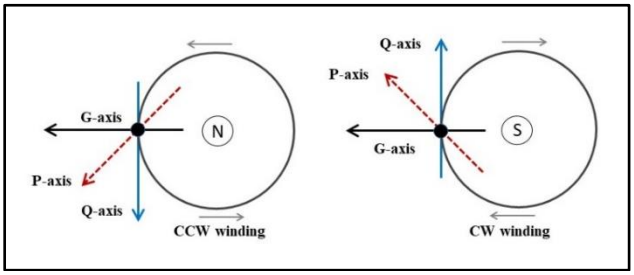

Above left, the electron Q-axes point down in the direction of current flow through the CCW winding. The inertial force on conduction electrons moving through the CCW winding aligns the direction of the electron G-axes to the left. The electron P-axes, perpendicular to both the Q-axes and P-axes, point S→N out of the paper.

Above right, the electron Q-axes point up in the direction of current flow through the CW winding. The inertial force on conduction electrons moving through the CW winding aligns the direction of the electron G-axes to the left. The electron P-axes, perpendicular to both the Q-axes and G-axes, point S→N into the paper.

Above is a turnbuckle composed of a metal frame tapped at each end. On the left end an LH bolt passes through an LH thread and on the right end an RH bolt passes through an RH thread. If the LH bolt is turned CCW (facing right into the turnbuckle frame) the bolt moves to the right and the frame moves to the left and if the LH bolt is turned CW the bolt moves to the left and the frame moves to the right. If the RH bolt is turned CW (facing left into the turnbuckle frame) the bolt moves to the left and the frame moves to the right and if the RH bolt is turned CCW the bolt moves to the right and the frame moves to the left.

In the language of this analogy, a graviton or quanton emitted by the emitting particle is a moving spinning bolt, and the absorbing particle is a turnbuckle frame with a G-axis, Q-axis or P-axis passing through.

In a chirality meshing interaction, absorption of a graviton or quanton by the LH or RH G-axis, Q-axis or P-axis of a particle, causes an attractive or repulsive acceleration proportional to the difference between the graviton or quanton velocity and the velocity of the absorbing particle.

An electron G-axis has a RH inside thread and a proton G-axis has a LH inside thread. An electron G-axis emits CW gravitons and a proton G-axis emits CCW gravitons.

In the bolt-turnbuckle analogy, a graviton is a moving spinning bolt, and the absorbing particle through which the G-axis passes is a turnbuckle frame:

- If a CCW graviton emitted by a proton is absorbed into a proton LH G-axis, the absorbing proton is attracted, accelerated in the direction of the emitting proton.
- If a CW graviton emitted by an electron is absorbed into an electron RH G-axis, the absorbing electron is attracted, accelerated in the direction of the emitting electron.

Protons and electrons do not gravitationally interact with each other because a proton is larger than an electron, a graviton emitted by a proton is larger than a graviton emitted by an electron, the inside thread of a proton G-axis is larger than the inside thread of an electron G-axis, and the size differences prevent the ability of a graviton emitted by an electron to mesh with a proton G-axis or a graviton emitted by a proton to mesh with an electron G-axis.

Tangible objects are composed of atoms which are composed of protons, electrons and neutrons. In gravitational interactions between tangible objects (with kilogram mass greater than one microgram or 1E20 particles) the total intensity of the interaction is the sum of the contributions of the electrons and protons of which the object is composed (note that neutrons themselves do not gravitationally interact but each neutron is composed of one electron and one proton both of which do gravitationally interact).

A particle Q-axis is a single-ended hollow cylinder. The mechanism of the Q-axis is analogous to a piston which moves up and down at a frequency proportional to charge intrinsic energy. At the end of each up-stroke a single quanton is emitted. The absorption window opens at the beginning of the up-stroke and remains open until the beginning of the downstroke or the absorption of a single quanton.

The difference (the intrinsic granularity) between the inside diameter of the hollow cylindrical Q-axis and the outside diameter of the quanton allows absorption of incoming quantons at angles that can deviate from normal (straight down the center) by plus or minus 20 arcseconds.

An electron Q-axis has a RH inside thread and a proton Q-axis has a LH inside thread. An electron Q-axis emits CCW quantons and a proton Q-axis emits CW quantons.

In the bolt-turnbuckle analogy, a quanton is a moving spinning bolt, and the absorbing particle through which the G-axis passes is a turnbuckle frame:

- If a CCW p-quanton emitted by a proton is absorbed into an electron RH Q-axis, the absorbing electron is attracted, accelerated in the direction of the emitting proton.
- If a CCW p-quanton emitted by a proton (or the anode plate in a CRT) is absorbed into a proton LH Q-axis, the absorbing proton is repulsed, accelerated in the direction of the cathode plate (opposite the direction of the emitting proton).
- If a CW e-quanton emitted by an electron is absorbed into an electron RH Q-axis, the absorbing electron is repulsed, accelerated in the direction opposite the emitting electron.
- If a CW e-quanton emitted by an electron (or the cathode plate in a CRT) is absorbed into a proton LH Q-axis, the absorbing proton is repulsed, accelerated in the direction of the cathode plate (the direction opposite the emitting electron).

In a CRT, the Q-axis of an accelerated electron is oriented in the linear direction of travel and its P-G-axis are oriented transverse to the linear direction of travel. After the electron is linearly accelerated, the electron passes between oppositely charged parallel plates that emit quantons perpendicular to the linear direction of travel and these e-quantons are absorbed into the electron P-axes. The chirality meshing interactions between an electron with a linear direction of travel and a quantons emitted by either plate results in a transverse acceleration in the direction of the anode plate:

- An incoming CCW p-quanton approaching an electron RH P-axis within less than 20 arcseconds deviation from normal (straight down the center) is absorbed in an attractive chirality meshing interaction in which the electron is deflected in the direction of the anode plate.
- An incoming CW e-quanton approaching an electron RH P-axis within less than 20 arcseconds deviation from normal (straight down the center) is absorbed in a repulsive chirality meshing interaction in which the electron is deflected in the direction of the anode plate.

This is the mechanism of the experimental determination of the electron-proton deflection ratio.

The magnitude of the ratio between these masses is not equal to the ratio of the measured gravitational deflections but rather to the inverse of the ratio of the measured electric deflections. It would not matter which of these measurable quantities were used in the experimental determination if Newton's laws of motion applied. However, in order for Newton's laws to apply the assumptions behind Newtons laws, specifically the 100% probability that particles gravitationally and electrically interact, must also apply. But this is not the case for action at a distance.

The electron orientation below top left, rotated 90 degrees CCW, is identical to the electron orientations previously illustrated for a CW disk generator or a CW-wound transformer or solenoid; and the electron orientation bottom left is a 180 degree rotation of top left.

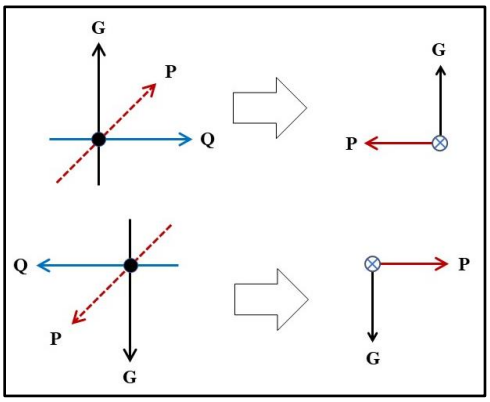

Above are reversals in Q-axis orientation due to reversals in direction of incoming quantons

Above top right and bottom right are the left-side electron orientations with the electron Q-axis directed into the plane of the paper (confirmation of the perspective transformation is easier to visualize with a model). These are the orientations of conduction electrons in an AC current.

In the top row CW quantons, emitted by the positive voltage source are absorbed in chirality meshing interactions by the electron RH Q-axis, attracting the absorbing electron. In the bottom row CCW quantons, emitted by the negative voltage source are absorbed in chirality meshing interactions into the electron RH Q-axis repelling the absorbing electron.

In either case the direction of current is into the paper.

In an AC current, a reversal in the direction of current is also a reversal in the rotational chirality of the quantons mediating the current.

- In a current moving in the direction of a positive voltage source each linear chirality meshing absorption of a CW p-quanton into an electron RH Q-axis results in an attractive deflection.
- In a current moving in the direction of a negative voltage source each linear chirality meshing absorption of a CCW e-quanton into an electron RH Q-axis results in a repulsive deflection.

In an AC current, each reversal in the direction of current, reverses the direction of the Q-axes of the conduction electrons. This reversal in direction is due to a complex rotation (two simultaneous 180 degree rotations) that results in photon emission.

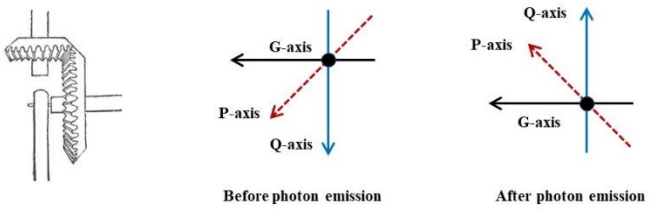

During a shorter or longer period of time (the inverse of the AC frequency) during which the direction of current reverses, a shorter or longer inductive pulse of electromagnetic energy flows into the electron Q and P axes and the quantons of which the electromagnetic energy is composed are absorbed in rotational chirality meshing interactions.

Above left, the electron P and Q axes mesh together at their mutual orthogonal origin in a mechanism analogous to a right angle bevel gear linkage.[8]

Above center and right, an incoming CCW quanton induces an inward CCW rotation in the Q-axis and causes a CW outward (CCW inward) rotation of the P-axis. The rotation of the Q-axis reverses the orientation of the P-axis and G-axis, and the rotation of the P-axis reverses the orientation of the Q-axis ***and*** the orientation of the G-axis thereby restoring its orientation to the initial direction pointing left and perpendicular to a tangent to the cylindrical wire.

Above center and right, an incoming CW quanton induces an inward CW rotation in the Q-axis and causes a CCW outward (CW inward) rotation of the P-axis. The rotation of the Q-axis reverses the orientation of the P-axis and G-axis, and the rotation of the P-axis reverses the orientation of the Q-axis ***and*** the orientation of the G-axis thereby restoring its orientation to the initial direction pointing left and perpendicular to a tangent to the cylindrical wire.

In either case the electron orientations are identical, but CCW electron rotations cause the emission of CCW photons and CW electron rotations cause the emission of CW photons.

The absorption of CCW e-quantons by the Q-axis rotates the Q-axis CCW by the square root of 648,000 arcseconds (180 degrees) and the P-Q axis linkage simultaneously rotates the P-axis CW by the square root of 648,000 arcseconds (180 degrees).

If the orientation of the electron G-axis is into the paper in a plane defined by the direction of the Q-axis, the CCW rotation of the Q-axis tilts the plane of the G-axis down by the square root of 648,000 arcseconds and the CW rotation of the P-axis tilts the plane of the G-axis to the right by the square root of 648,000 arcseconds.

The net rotation of the electron G-axis is equal to the product of the square root of 648,000 arcseconds and the square root of 648,000 arcseconds.

$$\text{Net rotation of the G-axis} = \left(\left(\sqrt{648,000}\right) x \left(\sqrt{648,000}\right)\right) = 648,000 \ \left(\text{arcseconds}\right) = 180 \ \left(\text{degrees}\right)$$

[8] Illustration from 1908 Chambers's Twentieth Century Dictionary. Public domain.

In the production of photons by an AC current, the photon wavelength and frequency are proportional to the current reversal time, and the photon energy is proportional to the voltage.

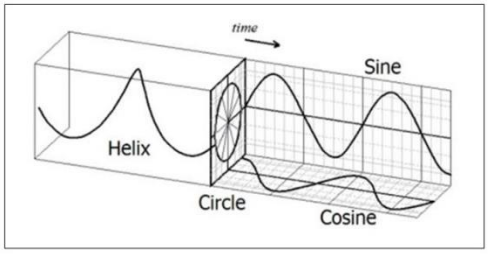

Above, an axial projection of the helical path of a photon traces the circumference of a circle and the sine and cosine are transverse orthogonal projections.[9] The crest to crest distance of the transverse orthogonal projections, or the distance between alternate crossings of the horizontal axis, is the photon wavelength.

The helical path of photons explains diffraction by a single slit, by a double slit, by an opaque circular disk, or a sphere (Arago spot).

In a beam of photons with velocity perpendicular to a flat screen or sensor, each individual photon makes a separate impact that can be sensed or is visible somewhere on the circumference of one of many separate and non-overlapping circles corresponding to all of the photons in the beam. The divergence of the beam increases the spacing between circles and the diameter of each individual photon circle which is proportional to the wavelength of each individual photon. The sensed or visible photon impacts form a region of constant intensity.

Below, the top image shows those photons, initially part of a photon beam illuminating a single slit, which passed through the single slit.[10]

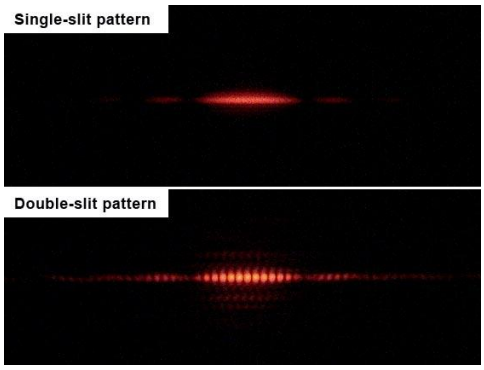

Above, the bottom image shows those photons, initially part of a photon beam illuminating a double slit, that passed through a double slit.

[9] Wikimedia “Sine and Cosine fundamental relationship to Circle and Helix” author Tdadamemd.
[10] By Jordgette - Own work, CC BY-SA 3.0, https://commons.wikimedia.org/w/index.php?curid=9529698

Below, the image illustrating classical rays of light passing through a double slit is equally illustrative of a photon beam illuminating a double slit but, instead of constructive and destructive interference, the photons passing through the top slit diverge to the right and photons passing through the bottom slit diverge to the left. The spaces between divergent circles are dark and, due to coherence, the photon circles are brightest at the distance of maximum overlap, resulting in the characteristic double slit brighter-darker diffraction pattern.[11]

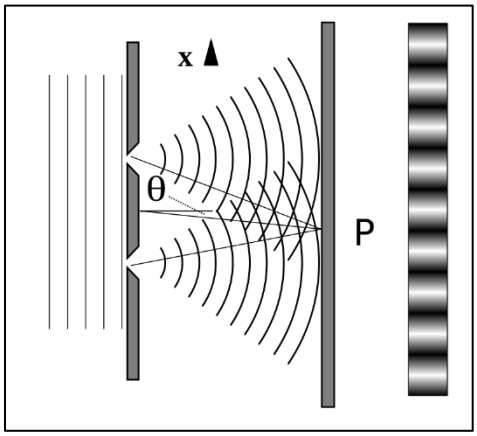

The mechanism of diffraction by an opaque circular disk or a sphere (Arago spot) is the same. In either case the opaque circular disk or sphere is illuminated by a photon beam of diameter larger than the diameter of the disk or sphere.

The photons passing close to the edge of the disk or sphere diverge inwards, and the spiraling helical path of a inwardly diverging CW photon passing one side of the disk will intersect in a head-on collision the spiraling helical path of a inwardly diverging CCW photon passing on the directly opposite side of the disk or sphere (if the opposite chirality photons are equidistant from the center of the disk or sphere).

In the case of a sphere illuminated by a laser, the surface of the sphere must be smooth and the ratio of the square of the diameter of the sphere divided by the product of the distance from the center of the sphere to the screen and the laser wavelength must be greater than one (similar to the Fresnel number).

$$\frac{d_S^2}{d_{screen}\lambda} > 1$$

[11] By Ebohr1.svg: en:User:Lacatosias, User:Stannereddderivative work: Epzcaw (talk) - Ebohr1.svg, CC BY-SA 3.0, https://commons.wikimedia.org/w/index.php?curid=15229922

Photon velocity

Constant photon velocity is due to a resonance driven by the emission of photon intrinsic energy which results in an increase in wavelength and a proportional decrease in frequency. In a related phenomenon, Arthur Holly Compton demonstrated Compton scattering in which the loss of photon kinetic energy does not change velocity but increases wavelength and proportionally decreases frequency.[12]

The mechanism of constant photon velocity is the emission of quantons and gravitons.

Below top, looking down into the plane of the paper a photon G-axis points in the direction of photon velocity and the P and Q-axes are orthogonal. In the language of the turnbuckle analogy, the mechanism of the photon P and Q-axes are analogous to pistons which move up and down or back and forth and emit a single quanton or graviton at the end of each stroke.

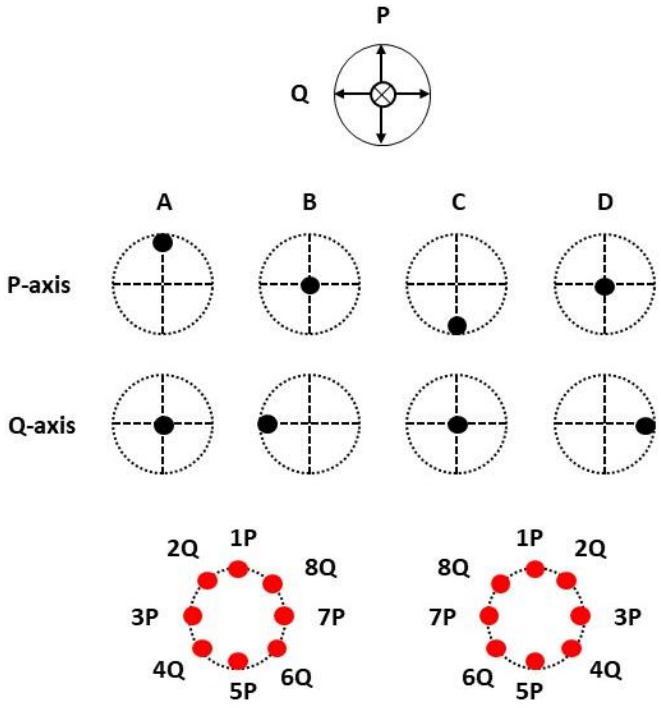

Above middle, in column A of the P-axis row, at the position of the oscillation the up-stroke has just completed, a single graviton has been emitted, and the current direction of the oscillation is now down. In column B of the P-axis row, the position of the oscillation is mid-way, and the direction of the oscillation is down. In column C of the P-axis row, at the position of the oscillation the downstroke has just completed, a single graviton has been emitted, and the current direction of the oscillation is up. In column D of the P-axis row, the position of the oscillation is mid-way, and the direction of the oscillation is up.

[12] https://www.nobelprize.org/prizes/physics/1927/summary/

Above middle, in column A of the Q-axis row, the position of the oscillation is mid-way and the direction of oscillation is left. In column B of the Q-axis row, at the position of the oscillation the left-stroke has just completed, a single quanton has been emitted, and the current direction of the oscillation is right. In column C of the Q-axis row, the position of the oscillation is mid-way and the direction of the oscillation is right. In column D of the Q-axis row, at the position of the oscillation the right-stroke has just completed, a single quanton has been emitted, and the current direction of the oscillation is left.

Above left or right bottom, in each cycle of the photon frequency there are eight sequential CCW or CW alternating quanton/graviton emissions and the intrinsic energy of the photon is reduced by *Lambda-bar* on each emission.

This is the mechanism of intrinsic redshift.

Part Three

Nuclear magnetic resonance

In the 1922 Stern-Gerlach experiment, a molecular beam of identical silver atoms passed through an inhomogeneous magnetic field. Contrary to classical expectations, the beam of atoms did not diverge into a cone with intensity highest at the center and lowest at the outside. Instead, atoms near the center of the beam were deflected with half the silver atoms deposited on a glass slide in an upper zone and half deposited in a lower zone, illustrating "space quantization."

The Stern-Gerlach experiment, designed to test directional quantization in a magnetic field as predicted by old quantum theory (the Bohr-Sommerfeld hypothesis)[13], was conducted two years before intrinsic spin was conceived by Wolfgang Pauli and six years before Paul Dirac formalized the concept. Intrinsic spin became part of the foundation of new quantum theory.

The concept of ***intrinsic*** spin, where the property that causes the deflection of silver atoms in two opposite directions "space quantization" is inherent in the particle itself, is incorrect.

However, a molecular beam composed of atoms with magnetic moments passed through a Stern-Gerlach apparatus does exhibit the numerical property attributed to intrinsic spin but this property, interactional spin, is not inherent in the atom but is dependent on external factors.

The protons within a nucleus are the origin of spin, magnetic moment, Larmor frequency, and other nuclear gyromagnetic properties. A nucleus contains "ordinary protons" which, for clarity, will be termed Pprotons, and "protons within neutrons" will be termed Nprotons.

In nuclei with an even number of Pprotons, the Pproton magnetic flux is contained within the nucleus and does not contribute to the nuclear magnetic moment.

With neutrons the situation is quite different. A neutron is achiral: it is a composite particle composed of an Nproton-electron pair and binding energy, it has no G-axis therefore does not gravitationally interact, and no Q-axis therefore is electrically neutral.

Within a nucleus, a neutron does not have a magnetic moment (during its less than 15-minute mean lifetime after a neutron is emitted from its nucleus, a free neutron has a measurable magnetic moment, but there are no free neutrons within nuclei) but the Nproton and electron of which a neutron is composed do have magnetic moments.

The gyromagnetic properties of a nucleus, its magnetic moment, its spin, its Larmor frequency, and its gyromagnetic ratio are due to Pprotons and Nprotons.

[13] O. Stern, Z. fur Physik, 7, 249 (1921), title in English: "A way to experimentally test the directional quantization in the magnetic field".

A molecular beam (composed of nuclei, atoms and/or molecules) emerging from an oven into a vacuum will have a thermal distribution of velocities. Molecules within the beam are subject to collisions with faster or slower molecules that cause rotations and vibrations, and the orientations of unpaired Pprotons and unpaired Nprotons are constantly subject to change.

In a silver atom there is a single unpaired Pproton and the orientation of its P-axis, with respect to its direction of motion through an inhomogeneous magnetic field, will be either leading or trailing. Out of a large number of unpaired Pprotons, the P-axes will be leading 50% of the time and trailing 50% of the time, and a silver atom containing an unpaired Pproton with a leading P-axis can be deflected in the direction of the inhomogeneous magnetic north pole while a silver atom containing an unpaired Pproton with a trailing P-axis can be deflected in the direction of the south pole.

If the magnetic field is strong enough for a sufficient percentage of unpaired Pprotons (the orientation of which is constantly changing) to encounter within 20 arcseconds lines of magnetic flux and be deflected up or down, the molecular beam of silver atoms deposited on a glass slide at the center of the magnetic field (where it is strongest) will be split into two zones and, consistent with the definition of spin as equal to the difference between the number of zones minus one divided by 2 (S = (z-1)/2), a Stern-Gerlach experiment determines a spin equal to ½. This result is the **only** example of spin clearly determined by the position of atoms deposited on a glass slide.[14]

The above explanation is correct for silver atoms passed through the inhomogeneous magnetic fields of the Stern-Gerlach apparatus, but in the 1939 Rabi experimental apparatus[15] (upon which modern molecular beam apparatus are modeled) the mechanism of deflection due to leading or trailing P-axes has nothing to do with the results achieved.

The 1939 Rabi experimental apparatus included back-to-back Stern-Gerlach inhomogeneous magnetic fields with opposite magnetic field orientations, but the result that dramatically changed physics, the accurate measurement of the Larmor frequency of nuclei, was done in a separate Rabi analyzer placed between the inhomogeneous magnetic fields. To Rabi, the importance of the Stern-Gerlach inhomogeneous magnets was for use in the alignment and tuning of the entire apparatus.

In a Rabi analyzer there is a strong constant magnetic field and a weaker transverse oscillating magnetic field. The purpose of the strong constant field is to decouple (increase the separation distance between) electrons and protons. The purpose of the transverse oscillating field is to stimulate the emission of photons by the decoupled protons.

When the Rabi apparatus is initially assembled, before installation of the Rabi analyzer the Stern-Gerlach apparatus is set up and tuned such that the intensity of the molecular beam leaving the apparatus is equal to its intensity upon entering.

---

[14] Ronald G. J. Fraser, Molecular Rays, Cambridge University Press, 1931.

[15] The Molecular Beam Resonance Method for Measuring Nuclear Magnetic Moments. II Rabi, S Millman, P Kusch, JR Zacharias - Physical review, 1939 - APS

After the unpowered Rabi analyzer is mounted between the Stern-Gerlach magnets, and the molecular beam exiting the first inhomogeneous magnetic field passes through the Rabi analyzer and enters the second inhomogeneous magnetic field, the intensity of the molecular beam leaving the apparatus decreases. In this state the entire Rabi apparatus is tuned and adjusted until the intensity of the entering molecular beam is equal to the intensity of the exiting beam.

When the crossed magnetic fields of the Rabi analyzer are switched on, for a second time the intensity of the exiting beam decreases. Then, by adjustment of the relative positions and orientations of the three magnetic fields (and also adjustment of the detector position to optimally align with decoupled protons *in the nucleus of interest*) the intensity of the exiting beam is returned to its initial value.

During an operational run, the transverse oscillating field stimulates the emission of photons at the same frequency as that of the transverse oscillating magnetic field. The ratio of the photon frequency divided by the strength of the strong magnetic field is equal to the Larmor frequency of the nucleus, and the Larmor frequency divided by the strong magnetic field strength is equal to the gyromagnetic ratio. The Larmor frequency has a very sharp resonant peak limited only by the accuracy of the two experimental measurables: the intensity of the strong magnetic field and the frequency of the oscillating weak magnetic field.

The gyromagnetic ratios of Li6, Li7, and F19, experimentally determined by Rabi in 1939, agree with the 2014 INDC[16] values to better than 1 part in 60,000. Importantly, measurements of the gyromagnetic ratios of Li6 and Li7 were made in three different lithium molecules (LiCl, LiF, and Li_2) requiring three separate operational runs, thereby demonstrating the Rabi analyzer was *adjusted to optimally detect the nucleus of interest*.

Modern determinations of spin are based on various types of spectroscopy, the results of which stand out as peaks in the collected data.

The magnetic flux of nuclei with an even number of Pprotons and Nprotons circulates in flux loops between pairs of Pprotons and pairs of Nprotons, and such nuclei do not have magnetic moments. The flux loops within nuclei with an odd number of Pprotons and/or Nprotons do have magnetic moments. In order for all nuclei of the same isotope to have zero or non-zero magnetic moments of the same amplitude, it is necessary for the magnetic flux loops to be circulating in the same plane.

All of the 106 selected magnetic nuclear isotopes from Lithium and Uranium, including all stable isotopes with atomic number (Z) greater than 2, plus a number of important isotopes with relatively long half-lives, belong to one of twelve different Types. The Type is determined based the spin of the isotope and the number of odd and even Pprotons and Nprotons.

An isotope contains an internal physical structure to which the property of magnetic moment correlates, but the magnetic moment is not entirely determined by the internal physical structure

[16] INDC: N. J. Stone 2014. Nuclear Data Section, International Atomic Energy Agency, www-nds.iaea.org/publications

of a nucleus. The property of interactional spin is that portion of the magnetic moment due to factors external to the nucleus, including electromagnetic radiation, magnetic fields, electric fields and excitation energy.

Of significance to the present discussion, the detectable magnetic properties of 82 of the 106 selected isotopes (the relative spatial orientations of the flux loops associated with the Pprotons and Nprotons) can be manipulated by four different orientations of directed planar electric fields.

The magnetic signatures of the 106 selected isotopes can be sorted into twelve isotope Types with seven spin values.

Spin ½ isotopes with an odd number of Pprotons and even number of Nprotons are Type A-0. Of the 106 selected isotopes, 10 are Type A-0.

Spin ½ isotopes with an even number of Pprotons and odd number of Nprotons (odd/even Reversed) are Type RA-0. Of the 106 selected isotopes, 14 are Type RA-0.

Spin 1 isotopes with an odd number of Pprotons and an odd number of Nprotons are Type B-1. Of the 106 selected isotopes, 2 are Type B-1.

Spin 3/2 isotopes with an odd number of Pprotons and even number of Nprotons are Type C-1. Of the 106 selected isotopes, 18 are Type C-1.

Spin 3/2 isotopes with an even number of Pprotons and odd number of Nprotons are Type RC-1. Of the 106 selected isotopes, 12 are Type RC-1.

Spin 5/2 isotopes with an odd number of Pprotons and even number of Nprotons are Type C-2. Of the 106 selected isotopes, 13 are Type C-2.

Spin 5/2 isotopes with an even number of Pprotons and odd number of Nprotons are Type RC-2. Of the 106 selected isotopes, 11 are Type RC-2.

Spin 3 isotopes with an odd number of Pprotons and an odd number of Nprotons are Type B-3. Of the 106 selected isotopes, 2 are Type B-3.

Spin 7/2 isotopes with an odd number of Pprotons and even number of Nprotons are Type A-3. Of the 106 selected isotopes, 9 are Type A-3.

Spin 7/2 isotopes with an even number of Pprotons and odd number of Nprotons are Type RA-3. Of the 106 selected isotopes, 8 are Type RA-3.

Spin 9/2 isotopes with an odd number of Pprotons and even number of Nprotons are Type C-4. Of the 106 selected isotopes, 3 are Type C-4.

Spin 9/2 isotopes with an even number of Pprotons and odd number of Nprotons are Type RC-4. Of the 106 selected isotopes, 4 are Type RC-4.

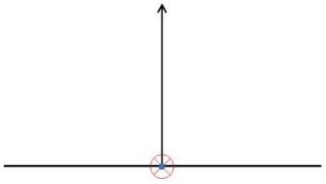

Above, the horizontal line is in the inspection plane. The vertical line, the photon path to the Rabi analyzer, is parallel to the constant magnetic field. The circle indicates the diameter of the molecular beam, and the crosshairs indicate the velocity of the beam is directed into the paper.

A molecular beam is not needed for the operation of a Rabi analyzer, all that is required is for an analytical sample (gas or liquid phase) comprising a large number of molecules containing a larger number of nuclei enclosing an even larger number of particles to be located at the intersection of the cross hairs.

The position of the horizontal inspection plane is irrelevant to Rabi analysis but it is crucial for spectroscopic analysis of flux loops.

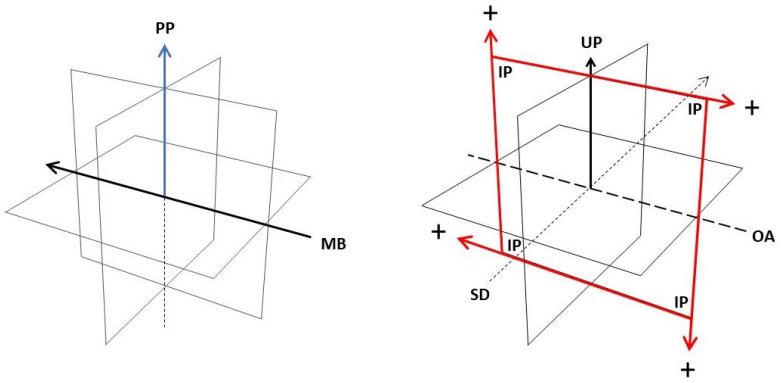

Above left, the molecular beam (directed into the paper in the previous illustration) is directed from right to left, and the photon path to the Rabi analyzer is in the same location as in the previous illustration.

For spectroscopic analysis, the inspection plane is the plane defined by the direction the molecular beam formerly passed and the direction of the positive electric field when pointing up.

Above right, the inspection plane for spectroscopic analysis, is labelled at each corner. The dashed line in place of the former position of the molecular beam is an orthogonal axis (OA) passing through the direction of the positive side of the electric field when pointing up (UP), and passing through the direction of the spectroscopic detectors (SD).

The intersection of OA, UP and SD is the location where the analytical sample (gas or liquid phase) is placed in the inspection plane. The electric field that orients particle Q-axes is in the inspection plane.

The detection of ten of the twelve Types of magnetic signatures (in the 106 selected isotopes) requires one of four alignments of directed electric fields: the positive side of the electric field pointing up, the positive side of the electric field pointing right, the positive side of the electric field pointing down, or the positive side of the electric field pointing left.

The four possible alignments of the electric field are illustrated on either side of the inspection plane (but in operation the entire breadth of the electric field points in the same direction) and the directed lines on the edges of the inspection plane represent the positions of thin wire cathodes that produce planar electric fields.

Prior to an operational run, the spectroscopic detectors are adjusted to optimally detect the magnetic properties of the isotope to be analyzed.

					
A-0					
RA-0					
B-1					
C-1					
RC-1					
C-2					
RC-2					
B-3					
A-3					
RA-3					
C-4					
RC-4					

Above is a summary of isotope magnetic signatures.

Column 1 lists the twelve magnetic isotope Types.

In column 2, with the P-axes of particles oriented by a constant magnetic field directed up in the direction of the magnetic north pole and in the absence of a directed electric field, the magnetic

signatures due to flipping odd Pproton P-axes (the arrow on the left of the vignette) and odd Nproton P-axes (the arrow on the right of the vignette) are illustrated.

See below, in the detailed discussion of Type B-1, for the reason there is a zero instead of an arrow in Types B-1 and B-3.

The magnetic signatures due to flux loops in the presence of the four orientations of an electric field, are given in columns 3, 4, 5 and 6 for electric fields directed up, directed down, directed to the right, or directed to the left.

In illustrations of flux loop magnetic signatures, if the arrows are oriented up and down the arrow on the left of the vignette represents the direction of Pproton flux loops and the arrow on the right represents the direction of Nproton flux loops, if the arrows are oriented left and right the arrow on the top of the vignette represents the direction of Pproton flux loops and the arrow on the bottom represents the direction of Nproton flux loops.

In total there are six directed orthogonal planes in Cartesian space but only four of these are represented in columns 3, 4, 5 and 6. This omission is due to the elliptical planar shape of magnetic flux loops: the missing orientations provide edge-on views without detectable magnetic signatures.

Type A-0

7N15, with 7 Pprotons and 8 Nprotons, is the lowest atomic number Type A-0 isotope. In Type A-0 isotopes the flux loops associated with Pprotons and Nprotons lie in a directed Cartesian plane without detectable flux loop signatures.

In an analytical sample, 50% of the odd (unpaired) Pproton P-axes will be oriented in one direction and 50% in the opposite direction. The orientation of the magnetic axes of the odd Pproton are flipped by the transverse oscillating magnetic field and the spectroscopic detectors sense two different magnetic signatures resulting in two peaks corresponding to a spin of ½.

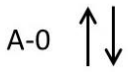

Above is the magnetic signature of Type A-0. The left arrow pointing up is the direction of the odd Pproton P-axis *after emission of a photon* (previously the constant magnetic field aligned the Pproton P-axis in this orientation, then absorption of intrinsic energy from the transverse oscillating magnetic field flipped the axis to pointing down then, due to the 180 degree rotation of the P-Q axes with respect to the direction of the G-axis, the absorbed intrinsic energy was released as a photon when the axis was flipped back to pointing up). The arrow pointing down is the antiparallel direction of the P-axis of a paired Nproton (which does not emit a photon).

The experimental detection of Type A-0 isotopes requires a constant magnetic field oriented in the direction of magnetic north.

Type RA-0

6C13, with 6 Pprotons and 7 Nprotons, is the lowest atomic number Type RA-0 isotope. In Type RA-0 isotopes the flux loops associated with Pprotons and Nprotons lie in a directed Cartesian plane without detectable flux loop signatures.

In an analytical sample, 50% of the odd (unpaired) Nproton P-axes will be oriented in one direction and 50% in the opposite direction. The orientation of the magnetic axes of the odd Nproton are flipped by the transverse oscillating magnetic field and the spectroscopic detectors produce two different magnetic signatures resulting in two peaks corresponding to a spin of ½.

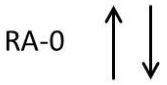

Above is the magnetic signature of Type RA-0. The left arrow pointing up is the direction of the P-axis of a paired Pproton (which does not emit a photon). The right arrow pointing down is the direction of the odd Nproton P-axis *after emission of a photon* (previously the constant magnetic field aligned the Nproton P-axis in this orientation, then absorption of intrinsic energy from the transverse oscillating magnetic field flipped the axis to pointing up then, due to the 180 degree rotation of the P-Q axes with respect to the direction of the G-axis, the absorbed intrinsic energy was released as a photon when the axis was flipped back to pointing down).

The experimental detection of Type RA-0 isotopes requires a constant magnetic field oriented in the direction of magnetic north.

Type B-1

3Li6, with 3 Pprotons and 3 Nprotons, is the lowest atomic number Type B-1 isotope. In isotopes with an odd number of Pprotons and Nprotons, the odd Pproton interacts with the electron in the odd Nproton preventing electron-Nproton decoupling by the constant magnetic field and the odd Nproton P-axis is unable to be flipped by the transverse oscillating magnetic field, but the electron-Pproton is decoupled and the orientation of the odd Pproton magnetic axis is flipped by the transverse oscillating magnetic field, and the spectroscopic detectors, adjusted to optimally recognize the magnetic signatures of 3Li6, sense one distinctive magnetic signature, resulting in one peak.

In Type B-1, the odd Nproton P-axis is unable to be flipped thus there is no magnetic signature due to the Nproton itself, but both the Nproton and the Pproton have associated flux loops and spectroscopic detectors can sense the magnetic signatures of the flux loops in the presence of a directed electric field pointing up.

In the analysis of isotopes with detectable flux loop signatures there are four possible orientations of the directed electric fields. The magnetic flux loops associated with Type-1 isotopes are detectable if the directed electric field is pointing up. The magnetic flux loops associated with Type-2 isotopes are detectable if the directed electric field is pointing down. The magnetic flux loops associated with Type-3 isotopes are detectable if the directed electric field is pointing right. The magnetic flux loops associated with Type-4 isotopes are detectable if the directed electric field is pointing left.

Each of these directed electric field orientations require different experiments, therefore the results of five experiments (including one experiment without directed electric fields) are needed to fully establish the Type of an unknown isotope.

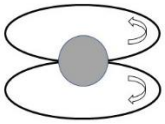

The flux loops circulating through particle P-axes can pass through all radial planes. The radial flux planes in the above diagram are in the plane of the paper demonstrating, when detected from opposite directions, flux loops will be CW (directed right-left) or CCW (directed left-right).

Since Pprotons and Nprotons are oppositely aligned, a CW Pproton signature is identical to an Nproton CCW signature, and a CCW Pproton signature is identical to an Nproton CW signature.

Because the magnetic signatures of the particles in the field of view of a detector are differently oriented, on average 50% of the flux loop magnetic signatures will be CW and 50% CCW. Of the 50% of the CW signatures 25% will be due to Pprotons and 25% due to Nprotons, and of the 50% of the CCW signatures 25% will be due to Pprotons and 25% due to Nprotons.

Thus, there will be two different magnetic signatures resulting to two peaks, but we are unable to distinguish which is due to CW Pproton flux loops or CCW Nproton flux loops, and which is due to CCW Pproton flux loops or CW Nproton flux loops.

In Type B-1, the magnetic signature due to the odd Pproton (experimentally determined in the absence of an electric field) has one peak, and the magnetic signature due to flux loops associated with Pprotons and Nprotons (experimentally determined in an electric field oriented parallel to the magnetic field) has two peaks, totaling three peaks corresponding to a spin of 1.

Here we come to a fundamental issue. Is the uncertainty in situations involving linked physical properties (complementarity) ***described*** by probability or is it ***caused*** by probability? In 1925 Werner Heisenberg theorized this type of uncertainty was ***caused*** by probability and that opinion became, along with intrinsic spin, an important part of the foundation of new quantum theory.

In nature, the orientation of the magnetic signatures of isotopes and the orientation of the nuclei containing the particles responsible for the magnetic signatures are random. The magnetic signatures due to a large number of randomly oriented particles are indistinguishable from background noise, but under the proper experimental conditions, the magnetic signatures are discernable.

The magnetic signatures of flux loops, imperceptible in nature, are perceptible when the Q-axes of the associated particles are aligned.

A constant magnetic field is not needed to detect the magnetic signatures of flux loops, but compared to the Rabi analyzer the inspection plane to detect the magnetic signatures of flux loops is in the identical position, and the directed orthogonal plane pointing up in the direction of magnetic north in the Rabi analyzer is the identical to the directed orthogonal plane pointing up in the direction of the positive electric field in the flux loops analyzer, that is, the direction of the electric field is parallel to the magnetic field.

Therefore, even though the magnetic field is not needed to detect the magnetic signatures of flux loops, if the magnetic field is present in addition to the directed electric field, its presence would not alter the experimental results, but it might provide additional information.

Here is a prediction of the present theory. If the experiment detecting the magnetic signature of Type B-1 is conducted in the presence of a constant magnetic field *and* a directed electric field pointing up, that one experiment will determine the magnetic signatures shown above plus two additional signatures: (1) the magnetic signature due to CW Pproton flux loops and CCW Nproton flux loops and (2) the magnetic signature due to CW Nproton flux loops and CCW Pproton flux loops.

This result would demonstrate the uncertainty in at least one situation involving linked physical properties is ***described*** by probability but is not ***caused*** by probability. This and other experiments yet to be devised, will overturn the concept of causation by probability, and validate Einstein's intuition that God "does not play dice with the universe."[17]

Type C-1

3Li7, with 3 Pprotons and 4 Nprotons, is the lowest atomic number Type C-1 isotope.

As in Type A-0, in a constant magnetic field absent electric fields the magnetic signature due to an odd particle has two peaks. As in Type B-1, the magnetic signature due to flux loops in a directed electric field pointing up has two peaks. In total, Type C-1 isotopes have four peaks corresponding to a spin of 3/2.

[17] "Quantum theory yields much, but it hardly brings us close to the Old One's secrets. I, in any case, am convinced He does not play dice with the universe." Letter from Einstein to Max Born (1926).

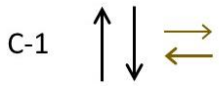

Type RC-1

4Be9, with 4 Pprotons and 5 Nprotons, is the lowest atomic number RC-1 isotope.

As in Type RA-0, in a constant magnetic field absent electric fields the magnetic signature due to an odd particle has two peaks. As in Type B-1, the magnetic signature due to flux loops in a directed electric field pointing up has two peaks. In total, Type RC-1 isotopes have four peaks corresponding to a spin of 3/2.

Type C-2

13Al27, with 13 Pprotons and 14 Nprotons, is the lowest atomic number Type C-2 isotope.

As in Type A-0, in a constant magnetic field absent electric fields the magnetic signature due to an odd particle has two peaks. As in Type B-1, the magnetic signature due to flux loops in a directed electric field pointing up has two peaks.

In the identification of Type C-2, the flux loops of an odd particle, determined in an electric field pointing down, has two peaks. In total, Type C-2 isotopes have six peaks corresponding to a spin of 5/2.

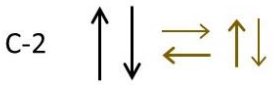

Type RC-2

8O17, with 8 Pprotons and 9 Nprotons, is the lowest atomic number Type RC-2 isotope. 8O17 has one odd Nproton and no odd Pprotons.

As in Type RA-0, in a constant magnetic field absent electric fields the magnetic signature due to an odd particle has two peaks. As in Type B-1, the magnetic signature due to flux loops in a directed electric field pointing up has two peaks.

In the identification of Type RC-2, the flux loops of an odd particle, determined in an electric field pointing down, has two peaks. In total, Type RC-2 isotopes have six peaks corresponding to a spin of 5/2.

RC-2 

Type B-3

5B10, with 5 Pprotons and 5 Nprotons, is the lowest atomic number Type B-3 isotope.

As in Type A-0, in a constant magnetic field absent electric fields the magnetic signature due to an odd particle has two peaks. As in Type B-1, the magnetic signature due to flux loops in a directed electric field pointing up has two peaks. As in Type C-2, the flux loops of an odd particle, determined in an electric field pointing down, has two peaks.

In the identification of Type B-3, the odd Pproton flux loops, determined in an electric field pointing right, has two peaks. In total, Type B-3 isotopes have seven peaks corresponding to a spin of 3.

B-3 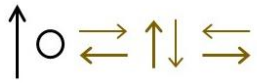

A-3

21Sc45, with 21 Pprotons and 24 Nprotons, is the lowest atomic number Type A-3 isotope.

As in Type A-0, in a constant magnetic field absent electric fields the magnetic signature due to an odd particle has two peaks. As in Type B-1, the magnetic signature due to flux loops in a directed electric field pointing up has two peaks. As in Type C-2, the flux loops of an odd particle, determined in an electric field pointing down, has two peaks. As in Type B-3, the magnetic signature due to flux loops in a directed electric field pointing right, has two peaks. In total, Type A-3 isotopes have eight peaks corresponding to a spin of 7/2.

A-3 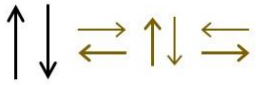

RA-3

20Ca43, with 20 Pprotons and 23 Nprotons, is the lowest atomic number Type RA-3 isotope.

As in Type RA-0, in a constant magnetic field absent electric fields the magnetic signature due to an odd particle has two peaks. As in Type B-1, the magnetic signature due to flux loops in a directed electric field pointing up has two peaks. As in Type RC-2, the flux loops of an odd particle, determined in an electric field pointing down, has two peaks. As in Type B-3, the

magnetic signature due to flux loops in a directed electric field pointing right, has two peaks. In total, Type RA-3 isotopes have 8 peaks corresponding to a spin of 7/2.

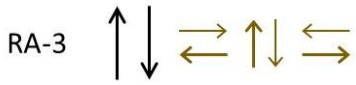

C-4

41NB93, with 41 Pprotons and 52 Nprotons, is the lowest atomic number Type C-4 isotope.

As in Type A-0, in a constant magnetic field absent electric fields the magnetic signature due to an odd particle has two peaks. As in Type B-1, the magnetic signature due to flux loops in a directed electric field pointing up has two peaks. As in Type C-2, the flux loops of an odd particle, determined in an electric field pointing down, has two peaks. As in Type B-3, the magnetic signature due to flux loops in a directed electric field pointing right, has two peaks. In the identification of Type C-4, the odd Nproton flux loops, determined in an electric field pointing left, has two peaks. In total, Type C-4 isotopes have 10 peaks corresponding to a spin of 9/2.

RC-4

32Ge73, with 32 Pprotons, 41 Nprotons, is the lowest atomic number Type RC-4 isotope.

As in Type RA-0, in a constant magnetic field absent electric fields the magnetic signature due to an odd particle has two peaks. As in Type B-1, the magnetic signature due to flux loops in a directed electric field pointing up has two peaks. As in Type RC-2, the flux loops of an odd particle, determined in an electric field pointing down, has two peaks. As in Type B-3, the magnetic signature due to flux loops in a directed electric field pointing right, has two peaks. In the identification of Type RC-4, the odd Nproton flux loops, determined in an electric field pointing left, has two peaks. In total, Type RC-4 isotopes have 10 peaks corresponding to a spin of 9/2.

	Z	N	Z+N	Spin	Peaks	Type
7N15	7	8	15	0.5	2	A-0
9F19	9	10	19	0.5	2	A-0
15P31	15	16	31	0.5	2	A-0
39Y89	39	50	89	0.5	2	A-0
45Rh103	45	58	103	0.5	2	A-0
47Ag109	47	62	109	0.5	2	A-0
47Ag107	47	60	107	0.5	2	A-0
69Tm169	69	100	169	0.5	2	A-0
81Tl203	81	122	203	0.5	2	A-0
81Tl205	81	124	205	0.5	2	A-0
6C13	6	7	13	0.5	2	RA-0
14Si29	14	15	29	0.5	2	RA-0
26Fe57	26	31	57	0.5	2	RA-0
34Se77	34	43	77	0.5	2	RA-0
48Cd111	48	63	111	0.5	2	RA-0
50Sn117	50	67	117	0.5	2	RA-0
50Sn115	50	65	115	0.5	2	RA-0
52Te125	52	73	125	0.5	2	RA-0
54Xe129	54	75	129	0.5	2	RA-0
74W183	74	109	183	0.5	2	RA-0
76Os187	76	111	187	0.5	2	RA-0
78Pt195	78	117	195	0.5	2	RA-0
80Hg199	80	119	199	0.5	2	RA-0
82Pb207	82	125	207	0.5	2	RA-0
3Li6	3	3	6	1.0	3	B-1
7N14	7	7	14	1.0	3	B-1
3Li7	3	4	7	1.5	4	C-1
5B11	5	6	11	1.5	4	C-1
11Na23	11	12	23	1.5	4	C-1
17Cl35	17	18	35	1.5	4	C-1
17Cl37	17	20	37	1.5	4	C-1
19K39	19	20	39	1.5	4	C-1
19K41	19	22	41	1.5	4	C-1
29Cu63	29	34	63	1.5	4	C-1
29Cu65	29	36	65	1.5	4	C-1
31Ga69	31	38	69	1.5	4	C-1
31Ga71	31	40	71	1.5	4	C-1
33As75	33	42	75	1.5	4	C-1
35Br79	35	44	79	1.5	4	C-1
35Br81	35	46	81	1.5	4	C-1
65Tb159	65	94	159	1.5	4	C-1
77Ir193	77	116	193	1.5	4	C-1
77Ir191	77	114	191	1.5	4	C-1
79Au197	79	118	197	1.5	4	C-1
4Be9	4	5	9	1.5	4	RC-1
10Ne21	10	11	21	1.5	4	RC-1
16S33	16	17	33	1.5	4	RC-1
24Cr53	24	29	53	1.5	4	RC-1
28Ni61	28	33	61	1.5	4	RC-1
54Xe131	54	77	131	1.5	4	RC-1
56Ba135	56	79	135	1.5	4	RC-1
56Ba137	56	81	137	1.5	4	RC-1
64Gd155	64	91	155	1.5	4	RC-1
64Gd157	64	93	157	1.5	4	RC-1

76Os189	76	113	189	1.5	4	RC-1
80Hg201	80	121	201	1.5	4	RC-1
13Al27	13	14	27	2.5	6	C-2
25Mn51	25	26	51	2.5	6	C-2
25Mn55	25	30	55	2.5	6	C-2
37Rb85	37	48	85	2.5	6	C-2
51Sb121	51	70	121	2.5	6	C-2
53I127	53	74	127	2.5	6	C-2
59Pr141	59	82	141	2.5	6	C-2
61Pm145	61	84	145	2.5	6	C-2
63Eu151	63	88	151	2.5	6	C-2
63Eu153	63	90	153	2.5	6	C-2
75Re185	75	110	185	2.5	6	C-2
8O17	8	9	17	2.5	6	RC-2
12Mg25	12	13	25	2.5	6	RC-2
22Ti47	22	25	47	2.5	6	RC-2
30Zn67	30	37	67	2.5	6	RC-2
40Zr91	40	51	91	2.5	6	RC-2
42Mo95	42	53	95	2.5	6	RC-2
42Mo97	42	55	97	2.5	6	RC-2
44Ru101	44	57	101	2.5	6	RC-2
44Ru99	44	55	99	2.5	6	RC-2
46Pd105	46	59	105	2.5	6	RC-2
66Dy161	66	95	161	2.5	6	RC-2
66Dy163	66	97	163	2.5	6	RC-2
70Yb173	70	103	173	2.5	6	RC-2
5B10	5	5	10	3.0	7	B-3
11Na22	11	11	22	3.0	7	B-3
21Sc45	21	24	45	3.5	8	A-3
23V51	23	28	51	3.5	8	A-3
27Co59	27	32	59	3.5	8	A-3
51Sb123	51	72	123	3.5	8	A-3
55Cs133	55	78	133	3.5	8	A-3
57La139	57	82	139	3.5	8	A-3
67Ho165	67	98	165	3.5	8	A-3
71Lu175	71	104	175	3.5	8	A-3
73Ta181	73	108	181	3.5	8	A-3
20Ca43	20	23	43	3.5	8	RA-3
22Ti49	22	27	49	3.5	8	RA-3
60Nd143	60	83	143	3.5	8	RA-3
60Nd145	60	85	145	3.5	8	RA-3
62Sm149	62	87	149	3.5	8	RA-3
68Er167	68	99	167	3.5	8	RA-3
72Hf177	72	105	177	3.5	8	RA-3
92U235	92	143	235	3.5	8	RA-3
41Nb93	41	52	93	4.5	10	C-4
49In113	49	64	113	4.5	10	C-4
83Bi209	83	126	209	4.5	10	C-4
32Ge73	32	41	73	4.5	10	RC-4
36Kr83	36	47	83	4.5	10	RC-4
38Sr87	38	49	87	4.5	10	RC-4
72Hf179	72	107	179	4.5	10	RC-4

	Z	N	Z+N	Spin	Peaks	Type
3Li6	3	3	6	1.0	3	B-1
3Li7	3	4	7	1.5	4	C-1
4Be9	4	5	9	1.5	4	RC-1
5B10	5	5	10	3.0	7	B-3
5B11	5	6	11	1.5	4	C-1
6C13	6	7	13	0.5	2	RA-0
7N14	7	7	14	1.0	3	B-1
7N15	7	8	15	0.5	2	A-0
8O17	8	9	17	2.5	6	RC-2
9F19	9	10	19	0.5	2	A-0
10Ne21	10	11	21	1.5	4	RC-1
11Na23	11	12	23	1.5	4	C-1
11Na22	11	11	22	3.0	7	B-3
12Mg25	12	13	25	2.5	6	RC-2
13Al27	13	14	27	2.5	6	C-2
14Si29	14	15	29	0.5	2	RA-0
15P31	15	16	31	0.5	2	A-0
16S33	16	17	33	1.5	4	RC-1
17Cl35	17	18	35	1.5	4	C-1
17Cl37	17	20	37	1.5	4	C-1
19K39	19	20	39	1.5	4	C-1
19K41	19	22	41	1.5	4	C-1
20Ca43	20	23	43	3.5	8	RA-3
21Sc45	21	24	45	3.5	8	A-3
22Ti47	22	25	47	2.5	6	RC-2
22Ti49	22	27	49	3.5	8	RA-3
23V51	23	28	51	3.5	8	A-3
24Cr53	24	29	53	1.5	4	RC-1
25Mn51	25	26	51	2.5	6	C-2
25Mn55	25	30	55	2.5	6	C-2
26Fe57	26	31	57	0.5	2	RA-0
27Co59	27	32	59	3.5	8	A-3
28Ni61	28	33	61	1.5	4	RC-1
29Cu63	29	34	63	1.5	4	C-1
29Cu65	29	36	65	1.5	4	C-1
30Zn67	30	37	67	2.5	6	RC-2
31Ga69	31	38	69	1.5	4	C-1
31Ga71	31	40	71	1.5	4	C-1
32Ge73	32	41	73	4.5	10	RC-4
33As75	33	42	75	1.5	4	C-1
34Se77	34	43	77	0.5	2	RA-0
35Br79	35	44	79	1.5	4	C-1
35Br81	35	46	81	1.5	4	C-1
36Kr83	36	47	83	4.5	10	RC-4
37Rb85	37	48	85	2.5	6	C-2
38Sr87	38	49	87	4.5	10	RC-4
39Y89	39	50	89	0.5	2	A-0
40Zr91	40	51	91	2.5	6	RC-2
41Nb93	41	52	93	4.5	10	C-4
42Mo95	42	53	95	2.5	6	RC-2
42Mo97	42	55	97	2.5	6	RC-2
44Ru101	44	57	101	2.5	6	RC-2
44Ru99	44	55	99	2.5	6	RC-2
45Rh103	45	58	103	0.5	2	A-0
46Pd105	46	59	105	2.5	6	RC-2
47Ag107	47	60	107	0.5	2	A-0

47Ag109	47	62	109	0.5	2	A-0
48Cd111	48	63	111	0.5	2	RA-0
49In113	49	64	113	4.5	10	C-4
50Sn115	50	65	115	0.5	2	RA-0
50Sn117	50	67	117	0.5	2	RA-0
51Sb121	51	70	121	2.5	6	C-2
51Sb123	51	72	123	3.5	8	A-3
52Te125	52	73	125	0.5	2	RA-0
53I127	53	74	127	2.5	6	C-2
54Xe129	54	75	129	0.5	2	RA-0
54Xe131	54	77	131	1.5	4	RC-1
55Cs133	55	78	133	3.5	8	A-3
56Ba135	56	79	135	1.5	4	RC-1
56Ba137	56	81	137	1.5	4	RC-1
57La139	57	82	139	3.5	8	A-3
59Pr141	59	82	141	2.5	6	C-2
60Nd143	60	83	143	3.5	8	RA-3
60Nd145	60	85	145	3.5	8	RA-3
61Pm145	61	84	145	2.5	6	C-2
62Sm149	62	87	149	3.5	8	RA-3
63Eu151	63	88	151	2.5	6	C-2
63Eu153	63	90	153	2.5	6	C-2
64Gd155	64	91	155	1.5	4	RC-1
64Gd157	64	93	157	1.5	4	RC-1
65Tb159	65	94	159	1.5	4	C-1
66Dy161	66	95	161	2.5	6	RC-2
66Dy163	66	97	163	2.5	6	RC-2
67Ho165	67	98	165	3.5	8	A-3
68Er167	68	99	167	3.5	8	RA-3
69Tm169	69	100	169	0.5	2	A-0
70Yb173	70	103	173	2.5	6	RC-2
71Lu175	71	104	175	3.5	8	A-3
72Hf177	72	105	177	3.5	8	RA-3
72Hf179	72	107	179	4.5	10	RC-4
73Ta181	73	108	181	3.5	8	A-3
74W183	74	109	183	0.5	2	RA-0
75Re185	75	110	185	2.5	6	C-2
76Os187	76	111	187	0.5	2	RA-0
76Os189	76	113	189	1.5	4	RC-1
77Ir191	77	114	191	1.5	4	C-1
77Ir193	77	116	193	1.5	4	C-1
78Pt195	78	117	195	0.5	2	RA-0
79Au197	79	118	197	1.5	4	C-1
80Hg199	80	119	199	0.5	2	RA-0
80Hg201	80	121	201	1.5	4	RC-1
81Tl203	81	122	203	0.5	2	A-0
81Tl205	81	124	205	0.5	2	A-0
82Pb207	82	125	207	0.5	2	RA-0
83Bi209	83	126	209	4.5	10	C-4
92U235	92	143	235	3.5	8	RA-3

In GAP, the gyromagnetic ratio of a nucleus is equal to the product of the INDC isotope g-factor and the CODATA nuclear magneton divided by the product of the INDC intrinsic spin and the CODATA reduced Plank constant, and the magnetic moment of a nucleus is equal to the product of the INDC isotope g-factor and the CODATA nuclear magneton.

$$\gamma_i = \frac{g_i \mu_N}{S_i \hbar} \quad \left(\frac{\text{Hz}}{\text{T}} = \frac{\text{C}}{\text{kg}} \right) \quad (\text{GAP})$$

$$u_i = g_i \mu_N \quad \left(\frac{\text{J}}{\text{T}} \right) \quad (\text{GAP})$$

In discrete physics, the magnetic moment of a nucleus is equal the product of two times the interactional spin (converts spin to number of odd Pprotons and/or odd Nprotons), the kinetic steric factor (converts molecular beam thermal energy into Joules), *Lambda-bar*, and the GAP value for the gyromagnetic ratio (assumed correct).

$$\mu_i = 2 S_i S_{\varnothing k} \lambda\!\!\!^{-} \gamma_i \quad \left(\frac{\text{J}}{\text{T}} \right) \quad (\text{discrete})$$

In the 106 isotopes tested, the ratio of the INDC isotope magnetic moment divided by the value denominated in discrete units is equal to 1.0288816.

$$\frac{\mu_i \ (\text{GAP})}{\mu_i \ (\text{discrete})} = 1.0288816$$

The difference can be narrowed by adjustment but cannot be eliminated because CODATA constants are not exactly reconciled.

Part Four

Particle acceleration

Einstein believed mass was constant and many of his revolutionary discoveries were based on that concept. Constancy of mass is an eminently reasonable assumption because Newtonian equations are also founded on mass conservation and in the majority of situations his equations accurately predict the observables. But in fact, as was succinctly expressed in his letter to Richard Bentley, his equations do not correspond to physical reality.[18]

Einstein also believed the speed of light was constant and since kinetic energy is proportional to mass and velocity, he concluded that the mass of a particle increases with velocity and approaches (but never reaches) a maximum value as the velocity approaches the speed of light. In special relativity he was able to derive, in a few simple equations, the relativistic momentum and energy (mass-energy) of a particle.

In general relativity, Einstein's field equations described the curvature of space-time in intense gravitational fields in agreement with the measured value for the precession of the perihelion of mercury. It seems likely the field equations were derived with that result in mind. Even so, this approach is eminently justifiable because measurables are valid assumptions for a physical theory.

Einstein's prediction that the curvature of space-time in intense gravitational fields was not only responsible for the precession of the perihelion of mercury but would also bend rays of light was verified in two astronomical expeditions led by Arthur Eddington and Andrew Crommelin. Their observations were acclaimed as verification of general relativity and today the curvature of space-time is considered by most scientists to be undisputed.

Unfortunately, this undisputed theory cannot determine the velocity of a relativistically accelerated electron or proton and does not provide a mechanism for the increase in energy and mass (mass-energy).

[18] "That gravity should be innate inherent & essential to matter so that one body may act upon another at a distance through a vacuum without the mediation of anything else by & through which their action or force may be conveyed from one to another is to me so great an absurdity that I believe no man who has … any competent faculty of thinking can ever fall into it." Original letter from Isaac Newton to Richard Bentley, 189.R.4.47, ff. 7-8, Trinity College Library, Cambridge, UK http://www.newtonproject.ox.ac.uk

The present theory derives the velocity and mass-energy of accelerated electrons and protons, and provides a mechanism.

In particle acceleration, charged particles are electrostatically formed into a linear beam and accelerated, then injected into a circular accelerator (or cyclotron) where they are magnetically formed into a circular beam and further accelerated by oscillating magnetic fields. Particle acceleration in linear and circular beams is mediated by chirality meshing interactions.

An electrostatic voltage is the emission of quantons:

- In electrostatic acceleration of negatively charged particles between a negative cathode on the left emitting CCW quantons and a positive anode on the right emitting CW quantons, chirality meshing absorptions of CCW quantons results in repulsive deflections (voltage acceleration) to the right and chirality meshing absorptions of CCW quantons results in attractive deflections (voltage acceleration) to the right.
- If positively charged particles are between a negative cathode on the left emitting CCW quantons and a positive anode on the right emitting CW quantons, chirality meshing absorptions of CW quantons results in attractive deflections (voltage acceleration) to the left and chirality meshing absorptions of CW quantons results in repulsive deflections (voltage acceleration) to the left.

Quantons are also produced transverse to a magnetic field with CCW quantons emitted by the magnetic North pole and CW quantons emitted by the magnetic South pole:

- In acceleration by a transverse oscillating magnetic field, charged particles are alternately pushed (repulsively deflected) from one direction and pulled (attractively deflected) from the opposite direction.
    - Negatively charged particles are alternately pushed (deflected in the direction of the positive anode) due to the absorption of CCW quantons and pulled (deflected in the direction of the positive anode) due to the absorption of CW quantons.
    - Positively charged particles are alternately pulled (deflected in the direction of the negative cathode) due to the absorption of CCW quantons, and pushed (deflected in the direction of the negative cathode) due to the absorption of CW quantons.

In either case (electrostatic voltage or oscillating magnetic voltage) the energy of simultaneous acceleration by oppositely directed voltages is proportional to the square of the voltage.

A chirality meshing absorption of a quanton increases the intrinsic energy of a particle and produces an intrinsic deflection that increases the particle velocity. Like kinetic acceleration, an intrinsic deflection increases the velocity but does so without the dissipation of kinetic energy.

The number of particles and quantons is directly proportional to the intrinsic Josephson constant: 3.0000E15 quantons are absorbed by 3.0000E15 particles per second per Volt. At 400 Volts 1.2000E18 quantons are absorbed by 1.2000E18 particles per second; and at 250,000 Volts 7.5000E20 quantons are absorbed by 7.5000E20 particles per second.

Each quanton absorption produces a deflection (acceleration) equal to the square root of *Lambda-bar* divided by the particle amplitude. Quanton absorption by an electron produces a deflection of 2.5327E-18 meters, and quanton absorption by a proton produces a deflection of 2.0680E-19 meters.

The number of chirality meshing interactions is equal to the square of the voltage divided by the square root of *Lambda-bar*. The intrinsic energy absorbed by a particle in a chirality meshing interaction is equal to the product of the number of chirality meshing interactions and *Lambda-bar*, divided by the number of particles. The accelerated particle intrinsic energy is equal to the sum of the particle intrinsic energy plus the intrinsic energy absorbed by the particle in a chirality meshing interaction.

The kinetic mass-energy in units of Joule is equal to the product of the accelerated particle intrinsic energy, the square of the photon velocity, and the ratio of the discrete Planck constant divided by *Lambda-bar*.

Electron acceleration

Below left, the GAP equation for electron velocity due to electrostatic or electromagnetic voltage is equal to the square root of the ratio of the product of 2, the CODATA elementary charge (units of Coulomb) and the voltage, divided by the CODATA electron mass (units of kilogram).

$$v_e = \sqrt{\frac{2\ e\ V}{m_e}}\ (\text{GAP}) \qquad v_e = \sqrt{\frac{2\ e_i\ V}{E_e}}\ (\text{discrete})$$

Above right, the discrete equation for electron velocity due to electrostatic or electromagnetic voltage is equal to the square root of the ratio of the product of 2, the charge intrinsic energy and the voltage, divided by the electron intrinsic energy.

The velocity calculated by the GAP equation is higher than the discrete equation by a factor of 1.007697. The difference can be narrowed by adjustment but cannot be eliminated because CODATA constants are not reconciled.

The analysis of electron acceleration includes a range of ten voltages between a minimum voltage and a maximum voltage. The maximum voltage is equal to a few millivolts less than the theoretical voltage required to accelerate an electron to the photon velocity (an impossibility), which, if calculated to fifteen significant digits, is 259807.621135332 Volts.

voltage	velocity	# electrons	def/q
1.0000000000E+00	5.8856619128E+05	3.0000000000E+15	2.5327856188E-18
1.0000000000E+02	5.8856619128E+06	3.0000000000E+17	2.5327856188E-18
4.0000000000E+02	1.1771323826E+07	1.2000000000E+18	2.5327856188E-18
8.0000000000E+02	1.6647165801E+07	2.4000000000E+18	2.5327856188E-18
4.0000000000E+03	3.7224194364E+07	1.2000000000E+19	2.5327856188E-18
1.0000000000E+04	5.8856619128E+07	3.0000000000E+19	2.5327856188E-18
2.5000000000E+04	9.3060485910E+07	7.5000000000E+19	2.5327856188E-18
1.0000000000E+05	1.8612097182E+08	3.0000000000E+20	2.5327856188E-18
2.5000000000E+05	2.9428309564E+08	7.5000000000E+20	2.5327856188E-18
2.59807621135E+05	3.0000000000E+08	7.7942286341E+20	2.5327856188E-18

# CMIs	delta IE/#e (E)	acc Ee (E)	mass-energy (J)
3.9482220389E+17	8.4426187295E-34	1.1195537298E-31	1.0471269286E-12
3.9482220389E+21	8.4426187295E-32	1.9553729841E-31	1.8288748923E-12
6.3171552622E+22	3.3770474918E-31	4.4881586029E-31	4.1978081156E-12
2.5268621049E+23	6.7540949836E-31	7.8652060947E-31	7.3563857467E-12
6.3171552622E+24	3.3770474918E-30	3.4881586029E-30	3.2625006795E-11
3.9482220389E+25	8.4426187295E-30	8.5537298406E-30	8.0003671262E-11
2.4676387743E+26	2.1106546824E-29	2.1217657935E-29	1.9845033243E-10
3.9482220389E+27	8.4426187295E-29	8.4537298406E-29	7.9068363826E-10
2.4676387743E+28	2.1106546824E-28	2.1117657935E-28	1.9751502499E-09
2.6650498762E+28	2.1934566883E-28	2.1945677994E-28	2.0525955817E-09

Top row column 1, the voltages used in this example analysis are 1, 100, 400, 800, 4000, 10000, 25000, 100000, 250000, and 259807.621135 Volts. The highest voltage, calculated to thirteen significant digits, exactly converts to the photon velocity (an impossibility) to eleven significant digits but is less than the photon velocity (the correct result) at 12 significant digits (this is an excellent example of a discretely exact property).

The equations following, calculations for 100 Volts, are identical to the equations for any other of the nine voltages, or for any other range of ten voltages greater than zero and less than the theoretical maximum.

Top row column 2, the calculated electron velocity per the discrete equation.

Top row column 3, the number of accelerated (deflected) electrons is equal to the ratio of the voltage divided by the intrinsic electron magnetic flux quantum.

$$\#e = \frac{V}{\Phi_{0ie}} = 3.000000x10^{17}$$

Top row column 4, the deflection per quanton is equal to the square root of *Lambda-bar* divided by the electron amplitude.

$$def\ /\ q = \frac{\sqrt{\lambda\!\!\!^{-}}}{a_e} = 2.532785x10^{-18}\ \ (\mathrm{m})$$

This is the deflection of a chirality meshing interaction between a quanton and an electron.

Bottom row column 1, the number of chirality meshing interactions is equal to the square of the voltage divided by the square root of *Lambda-bar*.

$$\#CMIs = \frac{V^2}{\sqrt{\lambda\!\!\!^{-}}} = 3.948222x10^{21}$$

Bottom row column 2, the increase in intrinsic energy per electron due to chirality meshing interactions, equal to the product of the number of chirality meshing interactions and *Lambda-bar* divided by the number of electrons, is denominated in units of Einstein.

$$\Delta IE\ /\ e\ = \frac{\#CMIs\ \lambda\!\!\!^{-}}{\#e} = 8.442618\mathrm{x}10^{-32}\ \ (\mathrm{E})$$

Bottom row column 3, the accelerated electron energy is equal to the sum of the electron intrinsic energy and the increase in intrinsic energy per electron.

$$acc\ E_e = E_e + (\Delta IE\ /\ e) = 1.955372x10^{-31}\ \ (\mathrm{E})$$

Bottom row column 4, the mass-energy in units of Joule is equal to the product of the accelerated electron intrinsic energy, the square of the photon velocity and the ratio of the discrete Planck constant divided by *Lambda-bar*.

$$mass\text{-}energy = acc\ E_e\ x\ c^2 x\left(\frac{h}{\lambda\!\!\!^{-}}\right) = 1.828874x10^{-12}\ (\mathrm{J})$$

Proton acceleration

The analysis of proton acceleration includes a range of ten voltages between a minimum voltage and a maximum voltage. For purposes of comparison, we specify the same voltages as used for the electron.

The theoretical voltage required to accelerate a proton to the photon velocity (an impossibility) is 38971143.1702997 Volts. Any voltage less than this theoretical maximum will accelerate a proton to less than the photon velocity.

The voltage range used in this example analysis is 1, 100, 400, 800, 4000, 10000, 25000, 100000, 250000, and 259807.621135 Volts. The equations below, the calculations for 100 Volts, are identical to the equations for any other accelerating voltage range greater than zero and less than the theoretical maximum.

The analysis of proton acceleration includes a range of ten voltages between a minimum voltage and a maximum voltage. The maximum voltage is equal to a few millivolts less than the theoretical voltage required to accelerate a proton to the photon velocity (an impossibility), which, if calculated to fifteen significant digits, is 259807.621135332 Volts.

Below left, the GAP equation for proton velocity due to electrostatic or electromagnetic voltage is equal to the square root of the ratio of the product of 2, the CODATA elementary charge (units of Coulomb) and the voltage, divided by the CODATA proton mass (units of kilogram).

$$v_p = \sqrt{\frac{2\ e\ V}{m_p}}\ (\text{GAP}) \qquad v_p = \sqrt{\frac{2\ e_i\ V}{E_p}}\ (\text{discrete})$$

Above right, the discrete equation for proton velocity, due to electrostatic or electromagnetic voltage, is equal to the square root of the ratio of the product of 2, the charge intrinsic energy (in units of intrinsic Volt) and the voltage, divided by the proton intrinsic energy (in units of Einstein).

The discrete proton velocity is lower than the discrete electron velocity by the square root of 150 (the square root of the proton amplitude).

The equations below, calculations for 100 Volts, are identical to the equations for any other of the nine voltages, or for any other range of ten voltages greater than zero and less than the theoretical maximum.

voltage	velocity	# protons	def/q
1.0000000000E+00	4.8056228283E+04	3.0000000000E+15	2.0680107980E-19
1.0000000000E+02	4.8056228283E+05	3.0000000000E+17	2.0680107980E-19
4.0000000000E+02	9.6112456565E+05	1.2000000000E+18	2.0680107980E-19
8.0000000000E+02	1.3592353959E+06	2.4000000000E+18	2.0680107980E-19
4.0000000000E+03	3.0393427426E+06	1.2000000000E+19	2.0680107980E-19
1.0000000000E+04	4.8056228283E+06	3.0000000000E+19	2.0680107980E-19
2.5000000000E+04	7.5983568565E+06	7.5000000000E+19	2.0680107980E-19
1.0000000000E+05	1.5196713713E+07	3.0000000000E+20	2.0680107980E-19
2.5000000000E+05	2.4028114141E+07	7.5000000000E+20	2.0680107980E-19
2.5980762000E+05	2.4494897374E+07	7.7942286000E+20	2.0680107980E-19

# CMIs	delta IE/#p (E)	acc Ep (E)	mass-energy (J)
3.9482220389E+17	8.4426187295E-34	1.6667510929E-29	1.5589246913E-10
3.9482220389E+21	8.4426187295E-32	1.6751092854E-29	1.5667421709E-10
6.3171552622E+22	3.3770474918E-31	1.7004371416E-29	1.5904315031E-10
2.5268621049E+23	6.7540949836E-31	1.7342076165E-29	1.6220172794E-10
6.3171552622E+24	3.3770474918E-30	2.0043714158E-29	1.8747034899E-10
3.9482220389E+25	8.4426187295E-30	2.5109285396E-29	2.3484901346E-10
2.4676387743E+26	2.1106546824E-29	3.7773213490E-29	3.5329567462E-10
3.9482220389E+27	8.4426187295E-29	1.0109285396E-28	9.4552898045E-10
2.4676387743E+28	2.1106546824E-28	2.2773213490E-28	2.1299955921E-09
2.6650498529E+28	2.1934566787E-28	2.3601233453E-28	2.2074409150E-09

Top row column 1, the voltages used in this example analysis are 1, 100, 400, 800, 4000, 10000, 25000, 100000, 250000, and 259807.621135 Volts. The highest voltage, calculated to thirteen significant digits, exactly converts to the photon velocity (an impossibility) to eleven significant digits but is less than the photon velocity (the correct result) at 12 significant digits.

The equations following, calculations for 100 Volts, are identical to the equations for any other of the nine voltages, or for any other range of ten voltages greater than zero and less than the theoretical maximum.

Top row column 2, the calculated proton velocity per the discrete equation.

Top row column 3, the number of accelerated (deflected) protons is equal to the ratio of the voltage divided by the intrinsic electron magnetic flux quantum.

$$\#\, p = \frac{V}{\Phi_{0ie}} = 3.000000x10^{17}$$

Top row column 4, the deflection per quanton is equal to the square root of *Lambda-bar* divided by the proton amplitude.

$$def\ /\ q = \frac{\sqrt{\lambda\!\!\!^{-}}}{a_p} = 2.0680107x10^{-19}\ \ (\mathrm{m})$$

This is the deflection of a chirality meshing interaction between a quanton and a proton.

Bottom row column 1, the number of chirality meshing interactions is equal to the square of the voltage divided by the square root of *Lambda-bar*.

$$\#CMIs = \frac{V^2}{\sqrt{\lambda\!\!\!^{-}}} = 3.948222x10^{21}$$

Bottom row column 2, the increase in intrinsic energy per proton due to chirality meshing interactions, equal to the product of the number of chirality meshing interactions and *Lambda-bar* divided by the number of protons, is denominated in units of Einstein.

$$\Delta IE\ /\ p\ = \frac{\#CMIs\ \lambda\!\!\!^{-}}{\#\,p} = 8.442618x10^{-32}\ \ (\mathrm{E})$$

Bottom row column 3, the accelerated proton energy is equal to the sum of the intrinsic proton energy and the increase in intrinsic energy per proton.

$$acc\ E_p = E_p + (\Delta IE\ /\ p) = 1.675109x10^{-29}\ \ (\mathrm{E})$$

Bottom row column 4, the mass-energy in units of Joule is equal to the product of the accelerated proton intrinsic energy, the square of the photon velocity and the ratio of the discrete Planck constant divided by *Lambda-bar*.

$$mass\text{-}energy = acc\ E_p\ x\ c^2 x\left(\frac{h}{\lambda\!\!\!^{-}}\right) = 1.566742x10^{-10}\,(\mathrm{J})$$

Part Five

Atomic Spectra

The Rydberg equations correspond to high accuracy with the hydrogen spectral series and the Newtonian equations correspond to high accuracy with orbital motion but, despite many years of considerable effort, physicists have been unable to account for the spectrum of helium or for non-Newtonian stellar rotation curves.

Previously, we reformulated the Newtonian equations and explained stellar rotation curves. In this chapter we will reformulate the Rydberg equations for the spectral series of hydrogen and derive a general explanation for atomic spectra.

The equation formulated by Johann Balmer in 1885, in which the hydrogen spectrum wave numbers are proportional to the product of a constant and the difference between the inverse square of two integers, is correct, but the Bohr Model is not.

The electron is not a point particle, the electron does not orbit the proton, the force conveyed by an electron is not transmitted an infinite distance, at an infinitesimal distance the force is not infinite, electrons with lower energy and lower wave number are closer to the proton, and electrons with higher energy and higher wave number are further away from the proton (**the Bohr distance-energy relationship must be reversed**).

In hydrogen an electron and proton are engaged in a positional resonance. In atoms larger than hydrogen many electrons and protons are engaged in positional resonances. Each resonance is between one electron external to the nucleus and one proton internal to the nucleus, in which the electron and the nuclear proton are facing in opposite directions and each particle emits quantons that are absorbed by the other particle. On emission by the electron the quanton is CCW and on emission by the nuclear proton the quanton is CW. On emission the emitting particle recoils by a distance proportional to the particle intrinsic energy and on absorption the absorbing particle is attractively deflected (a chirality meshing interaction) by a distance proportional to the particle intrinsic energy. The result is a sustained positional resonance of a CCW quanton emitted in one direction by the electron and absorbed by the nuclear proton and a CW quanton emitted in the opposite direction by the nuclear proton and absorbed by the electron.

In the hydrogen atom, the resonance can be situated at any one of several quantized positions proportional to energy and corresponding to spectral emission and absorption lines. On emission of a photon the energy of the resonance decreases, and the electron drops to the adjacent lower energy level. On absorption of a photon the energy of the resonance increases, and the electron jumps to the adjacent higher energy level. The highest stable energy level, corresponding to an emission-only line, the maximum electron-proton separation distance beyond which the positional resonance no longer exists, is the hydrogen ionization energy.

The above paragraphs summarize the spectral mechanism which, for the time being, shall be considered a hypothesis.

The intrinsic to kinetic energy factor is equal to the ratio of the discrete Planck constant divided by the Coulomb divided by the ratio of *Lambda-bar* divided by the charge intrinsic energy, the ratio of the discrete Planck constant divided by the product of *Lambda-bar* and the square root of the proton amplitude divided by two, and two times the intrinsic steric factor.

$$F\left(IE \rightarrow KE\right) = \frac{\left(h/e_c\right)}{\left(\lambda\!\!\!^{-}/e_i\right)} = \frac{h}{\lambda\!\!\!^{-}\sqrt{a_p/2}} = 2S_{\varnothing i} = 12$$

The ionization energy of hydrogen (in larger atoms the ionization energy required to remove the last electron) is a discretely exact single value above which the atom no longer exists. The measured energy of hydrogen ionization is 1312 kJ/mol, and the corresponding CRC value is 13.59844 (units of kinetic electron Volts).[19] Kinetic electron Volts divided by *Omega-2* equals intrinsic Volts (units of Joule), which divided by 12 (the intrinsic to kinetic energy factor) equals intrinsic Volts (units of Einstein), which multiplied by the intrinsic electron charge equals intrinsic energy, which divided by *Lambda-bar* is equal to the photon frequency of hydrogen ionization.

Working backwards from the calculation sequences above, the discretely exact value of the photon ionization frequency is 3.28000000E15.

$$f_{ph} = 3.28000000x10^{15} \ \left(\mathrm{Hz}\right)$$

The intrinsic energy of hydrogen ionization, denominated in units of Einstein, is equal to the product of the photon frequency and *Lambda-bar*.

$$f_{ph}\lambda\!\!\!^{-} = 2.10412098x10^{-20}\left(\mathrm{E}\right)$$

The intrinsic energy of hydrogen ionization, denominated in units of Joule, is equal to the product of the photon frequency and the discrete Planck constant.

$$f_{ph}h = 2.18666666x10^{-18}\left(\mathrm{J}\right)$$

The intrinsic voltage of hydrogen ionization, denominated in units of Einstein, is equal to the product of the photon frequency and *Lambda-bar*, divided by the charge intrinsic energy.

$$V_{i(E)} = \frac{f_{ph}\lambda\!\!\!^{-}}{e_i} = 1.09333333 \ \left(\mathrm{E}\right)$$

[19] Ionization energies of the elements (data page), https://en.wikipedia.org/

The ratio of the intrinsic voltage of hydrogen ionization divided by *Psi* is equal to the discrete Rydberg constant and denominated in units of inverse meter (spatial frequency).

$$R_y = \frac{V_{i(E)}}{\psi} = 1.09333333x10^7 \ \left(\mathrm{m}^{-1}\right)$$

The intrinsic voltage of hydrogen ionization, denominated in units of Joule, is equal to the product of 12 (the intrinsic to kinetic energy factor) and the discrete Rydberg constant, and the product of the photon frequency and the discrete Planck constant, divided by the Coulomb.

$$V_{i(J)} = 12R_y = \frac{f_{ph}h}{e_c} = 13.12000000 \ \left(\mathrm{J}\right)$$

The kinetic voltage of hydrogen ionization, denominated in units of electron Volt, is equal to the product of the intrinsic voltage of hydrogen ionization and *omega-2*.

$$V_{k(eV)} = V_{i(J)}\omega^2 = 13.63470395 \ \left(\mathrm{eV}\right)$$

The difference between the above calculated energy of ionization and the CRC value is less than 0.30%. The poor accuracy is due to the performance standards of calorimeters.[20] In the measurement of a sample against a calibration standard, a statistical analysis of the results will show the data lie within three standard deviations (sigma-3) of the mean (the expected value) and the accuracy will be 0.15% (99.85% of the measurements will lie in the range of higher than the calibration standard by no more than 0.15% or lower than the calibration standard by no more than 0.15%). If the identical procedure is used without prior knowledge of the expected result and whether the measurement is higher or lower than the actual value is unknown, the accuracy falls to no more than 0.30%.

$$\frac{13.634703}{13.598440} = 1.002666$$

The calculated value of the kinetic voltage of hydrogen ionization divided by the measured CRC value, expressed as a percentage, is 0.2666%.

Spectral series consist of a number of emission-absorption lines with a lower limit on the left and an upper limit on the right. Both limits are asymptotes: the lower limit corresponds to minimum energy, minimum frequency, and maximum wavelength; and the upper limit corresponds to maximum energy, maximum frequency, and minimum wavelength.

The below diagram of the Lyman spectral series consists of seven black emission-absorption lines to the left and a red emission-only line on the right. From left to right these lines are the

[20] How to determine the range of acceptable results for your calorimeter, Bulletin No. 100, Parr Instrument Company, www.parrinst.com.

Lyman lower limit (Lyman-A), Lyman-B, Lyman-C, Lyman-D, Lyman-E, Lyman-F, Lyman-G, and the Lyman upper limit.

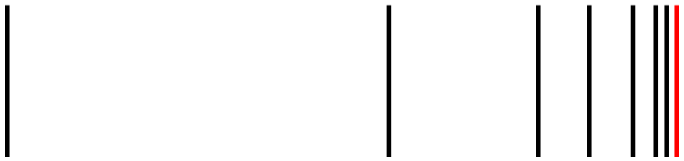

The Rydberg equation expresses the wave numbers of the hydrogen spectrum equal to the product of the discrete Rydberg constant and the difference between the inverse square of the m-index minus the inverse square of the n-index.

$$wn = R_y\left(\left(\frac{1}{m^2}\right)-\left(\frac{1}{n^2}\right)\right) \quad \left(\mathrm{m}^{-1}\right)$$

The m-index has a constant value for each spectral series within the hydrogen spectrum. The six series ordered by highest energy (at the series upper limit) are Lyman, Balmer, Paschen, Brackett, Pfund and Humphreys.

Each line of a spectral series can be expressed in terms of energy, wave number, wavelength and photon frequency. The energy, wave number, and frequency increase from left to right, but the wavelength decreases from left to right.

For each spectral series the m-index increases from lowest to highest positional energy (Lyman = 1, Balmer = 2, Paschen = 3, Brackett = 4, Pfund = 5, Humphreys = 6). Each spectral series is composed of a sequence of lines (A, B, C, D, E, F, G) in which the n-index is equal to m+1, m+2, m+3, m+4, etc.

In the following analysis we will apply the Rydberg formula to calculate, based on the discretely exact value of the photon ionization frequency of 3.280000E15, the values for energy, wave number and frequency of the six spectral series of hydrogen.

The below calculations begin with the discretely exact values for the Lyman limit photon frequency and the hydrogen ionization energy (intrinsic voltage units of Joule), and the value of the discrete Rydberg constant.

The Lyman upper limit is an emission-only line because at any energy above the Lyman upper limit the hydrogen atom no longer exists. The calculation for the line prior to the Lyman upper limit is based on an n-index equal to 8, but there are additional discernable lines after Lyman-G because the Lyman upper limit is an asymptote. The identical situation holds for the limit of any spectral series.

The spectral series lower limit, the A-line (Lyman-A, Balmer-A, etc.) is also an asymptote and there are additional discernable lines between the C-line and the A-line. The number of lines included in a spectral series analysis is optional, but it is convenient to use the same number of lines in spectral series to be compared.

In this presentation, 8 Lyman and Balmer lines are included because these lines are specified in at least one of the easily available online sources. In the Paschen, Brackett, Pfund and Humphreys spectral series, 6 lines are included because these are also easily available.[21]

The ratio of the Lyman upper limit divided by the upper limit of another hydrogen spectral series is equal to the square of the m-index of the other series:

- The Lyman upper limit divided by the Balmer upper limit is equal to 4.
- The Lyman upper limit divided by the Paschen upper limit is equal to 9.
- The Lyman upper limit divided by the Brackett upper limit is equal to 16.
- The Lyman upper limit divided by the Pfund upper limit is equal to 25.
- The Lyman upper limit divided by the Humphreys upper limit is equal to 36.

The ratio of the Lyman spectral series upper limit divided by the Lyman spectral series lower limit is equal to the ratio of the Rydberg wave number calculation for the upper limit divided by the Rydberg wave number calculation for the lower limit.

$$\frac{Ry\left(\frac{1}{m^2}-\frac{1}{n^2}\right)\ (\text{Lyman upper limit})}{Ry\left(\frac{1}{m^2}-\frac{1}{n^2}\right)\ (\text{Lyman lower limit})}=\frac{4}{3}=1.333333$$

In all spectral series the Rydberg ratio is equal to the upper limit energy divided by the lower limit energy, the ratio of the upper limit structural frequency divided by the lower limit structural frequency, and the ratio of the *lower limit wavelength divided by the upper limit wavelength*.

The ratio of the Balmer spectral series upper limit divided by the Balmer spectral series lower limit is equal to the ratio of the Rydberg wave number calculation for the upper limit divided by the Rydberg wave number calculation for the lower limit.

$$\frac{Ry\left(\frac{1}{m^2}-\frac{1}{n^2}\right)\ (\text{Balmer upper limit})}{Ry\left(\frac{1}{m^2}-\frac{1}{n^2}\right)\ (\text{Balmer lower limit})}=\frac{77}{45}=1.711111$$

The same calculation is used for the other four hydrogen spectral series:

- The ratio of the Paschen spectral series upper limit divided by the Paschen lower limit is equal to 1312/574 (2.285714).
- The ratio of the Brackett spectral series upper limit divided by the Brackett lower limit is equal to 25/9 (2.777777).

[21] See www.wikipedia.org, www.hyperphysics.com, www.shutterstock.com

- The ratio of the Pfund spectral series upper limit divided by the Pfund lower limit is equal to 36/11 (3.272727).
- The ratio of the Humphreys spectral series upper limit divided by the Humphreys lower limit is equal to 3.769230.

Lyman	A	B-A	B	C-B	C	D-C	D
m	1		1		1		1
n	2		3		4		5
energy Vi (J)	9.840000	1.822222	11.662222	0.637778	12.300000	0.295200	12.595200
wn	8.200000E+06	1.518519E+06	9.718519E+06	5.314815E+05	1.025000E+07	2.460000E+05	1.049600E+07
wl calc	1.219512E-07		1.028963E-07		9.756098E-08		9.527439E-08
Freq	2.460000E+15	**4.555556E+14**	2.915556E+15	**1.594444E+14**	3.075000E+15	**7.380000E+13**	3.148800E+15
wl meas	1.215700E-07		1.215700E-07		1.215700E-07		1.215700E-07
wl calc/meas	1.003136E+00		8.463958E-01		8.025086E-01		7.836998E-01

Lyman	E-D	E	F-E	F	G-F	G	Limit
m		1		1		1	1
n		6		7		8	1000000
energy Vi (J)	0.160356	12.755556	0.096689	12.852245	0.062755	12.915000	13.120000
wn		1.062963E+07		1.071020E+07		1.076250E+07	1.093333E+07
wl calc		9.407666E-08		9.336890E-08		9.291521E-08	9.146341E-08
Freq	**4.008889E+13**	3.188889E+15	**2.417234E+13**	3.213061E+15	**1.568878E+13**	3.228750E+15	3.280000E+15
wl meas		9.378000E-08		9.307000E-07		9.260000E-08	9.117500E-08
wl calc/meas		1.003163E+00		1.003212E-01		1.003404E+00	1.003163E+00

Balmer	A	B-A	B	C-B	C	D-C	D
m	2		2		2		2
n	3		4		5		6
energy Vi (J)	1.822222	0.637778	2.460000	0.295200	2.755200	0.160356	2.915556
wn	1.518519E+06	5.314815E+05	2.050000E+06	2.460000E+05	2.296000E+06	1.336296E+05	2.429630E+06
wl calc	6.585366E-07		4.878049E-07		4.355401E-07		4.115854E-07
Freq	**4.555556E+14**	**1.594444E+14**	6.150000E+14	**7.380000E+13**	6.888000E+14	**4.008889E+13**	7.288889E+14
wl meas	6.562790E-07		4.861350E-07		4.340472E-07		4.101734E-07
wl calc/meas	1.003440		1.003435		1.003439		1.003442

Balmer	E-D	E	F-E	F	G-F	G	Limit
m		2		2		2	2
n		7		8		9	1000000
energy Vi (J)	3.012245	3.012245	0.062755	3.075000	0.043025	3.118025	3.280000
wn	8.057445E+04	2.510204E+06	5.229592E+04	2.562500E+06	3.585391E+04	2.598354E+06	2.733333E+06
wl calc		3.983740E-07		3.902439E-07		3.848590E-07	3.658537E-07
Freq	**2.417234E+13**	7.530612E+14	**1.568878E+13**	7.687500E+14	1.075617E+13	7.795062E+14	8.200000E+14
wl meas		3.970075E-07		3.889064E-07		3.835397E-07	3.646000E-07
wl calc/meas		1.003442		1.003439		1.003440	1.003438

Above, the frequencies under the A, B, C, D, E, F, G-lines and the series limit are the positional structural frequencies, and the transition frequencies between lines (B-A, C-B … F-E, G-F) are the photon emission-absorption frequencies.

The structural frequency of the G-line is equal to the product of the Rydberg calculated wave number and the photon velocity. The energy of the G-line (intrinsic Volts units of Joule) is equal to the product of the structural frequency of the G-line and the Coulomb divided by the discrete Planck constant.

The structural frequency of the F-line is equal to the product of the Rydberg calculated wave number and the photon velocity. The energy of the F-line (intrinsic Volts units of Joule) is equal to the product of the structural frequency of the F-line and the Coulomb divided by the discrete Planck constant.

The photon emission-absorption frequency of the G-F transition is equal to the structural frequency of the G-line minus the structural frequency of the F-line. The energy of the G-F transition (intrinsic Volts units of Joule) is equal to the energy of the G-line minus the energy of the F-line.

The identical process is used to calculate the emission-absorption frequencies and energies for all spectral series.

Note there is no transition frequency or energy between the G-line and the series limit because the series limit is emission-only.

Lyman series transition photons identical to Balmer series photons:

- When a Lyman-C positional resonance drops down to Lyman-B, the Lyman-C energy is emitted as two photons: a 11.662222 Vi(J) Lyman-B photon frequency 2.915555E15 and a 0.637777 Vi(J) Lyman C-B photon frequency 1.594444E14. The frequency and wavelength of the transition photon is identical to the Balmer B-A transition photon.
- When a Lyman-D positional resonance drops down to Lyman-C, the Lyman-D energy is emitted as two photons: a 12.300000 Vi(J) Lyman-C photon frequency 3.075000E15 and a 0.295200 Vi(J) Lyman D-C photon frequency 7.380000E13. The frequency and wavelength of the transition photon is identical to the Balmer C-B transition photon.
- When a Lyman-E positional resonance drops down to Lyman-D, the Lyman-E energy is emitted as two photons: a 12.595200 Vi(J) Lyman-D photon frequency 3.148800E15 and a 0.160356 Vi(J) Lyman E-D photon frequency 4.008888E13. The frequency and wavelength of the transition photon is identical to the Balmer D-C transition photon.
- When a Lyman-F positional resonance drops down to Lyman-E, the Lyman-F energy is emitted as two photons: a 12.755555 Vi(J) Lyman-E photon frequency 3.188888E15 and a 0.096689 Vi(J) Lyman F-E photon frequency 2.41723E13. The frequency and wavelength of the transition photon is identical to the Balmer E-D transition photon.
- When a Lyman-G positional resonance drops down to Lyman-F, the Lyman-G energy is emitted as two photons: a 12.852245 Vi(J) Lyman-F photon frequency 3.21306E15 and a 0.062755 Vi(J) Lyman G-F photon frequency 1.568878E13. The frequency and wavelength of the transition photon is identical to the Balmer F-E transition photon.

The equivalence of Balmer-A and Lyman series transitions can be extended to the Paschen, Brackett, Pfund and Humphreys series.

The Lyman C-B transition is equal to the energy and frequency of Paschen-A.

Paschen	A	B	C	D	E	Limit
m	3	3	3	3	3	3
n	4	5	6	7	8	1000000
Energy (eV)	0.63777778	0.93297778	1.09333333	1.19002268	1.25277778	1.45777778
freq	1.59444444E+14	2.33244444E+14	2.73333333E+14	2.97505669E+14	3.13194444E+14	3.64444444E+14
wl calc	1.88153310E-06	1.28620427E-06	1.09756098E-06	1.00838415E-06	9.57871397E-07	8.23170732E-07
wl meas	1.87500000E-06	1.28200000E-06	1.09400000E-06	1.00500000E-06	9.54600000E-07	8.20400000E-07
wl calc/meas	1.00348432	1.00327946	1.00325501	1.00336731	1.00342698	1.00337729

The Lyman D-C transition is equal to the energy and frequency of Brackett-A.

Brackett	A	B	C	D	E	Limit
m	4	4	4	4	4	4
n	5	6	7	8	9	1000000
Energy (eV)	0.29520000	0.45555556	0.55224490	0.61500000	0.65802469	0.82000000
freq	7.38000000E+13	1.13888889E+14	1.38061224E+14	1.53750000E+14	1.64506173E+14	2.05000000E+14
wl calc	4.06504065E-06	2.63414634E-06	2.17294900E-06	1.95121951E-06	1.82363977E-06	1.46341463E-06
wl meas	4.05100000E-06	2.62500000E-06	2.16600000E-06	1.94400000E-06	1.81700000E-06	1.45800000E-06
wl calc/meas	1.00346597	1.00348432	1.00320822	1.00371374	1.00365425	1.00371374

The Lyman E-D transition is equal to the energy and frequency of Pfund-A.

Pfund	A	B	C	D	E	Limit
m	5	5	5	5	5	5
n	6	7	8	9	10	1000000
Energy (eV)	0.16035556	0.25704490	0.31980000	0.36282469	0.39360000	0.52480000
freq	4.00888889E+13	6.42612245E+13	7.99500000E+13	9.07061728E+13	9.84000000E+13	1.31200000E+14
wl calc	7.48337029E-06	4.66844512E-06	3.75234522E-06	3.30738240E-06	3.04878049E-06	2.28658537E-06
wl meas	7.46000000E-06	4.65400000E-06	3.74100000E-06	3.29700000E-06	3.03000000E-06	2.27900000E-06
wl calc/meas	1.00313275	1.00310381	1.00303267	1.00314905	1.00619818	1.00332837

The Lyman F-E transition is equal to the energy and frequency of Humphreys-A.

Humphreys	A	B	C	D	E	Limit
m	6	6	6	6	6	6
n	7	8	9	10	11	1000000
Energy (eV)	0.09668934	0.15944444	0.20246914	0.23324444	0.26342975	0.36444444
freq	2.41723356E+13	3.98611111E+13	5.06172840E+13	5.83111111E+13	6.58574380E+13	9.11111111E+13
wl calc	1.24108818E-05	7.52613240E-06	5.92682927E-06	5.14481707E-06	4.68723099E-06	3.29268293E-06
wl meas	1.23700000E-05	7.50300000E-06	5.90800000E-06	5.12900000E-06	4.67300000E-06	3.28200000E-06
wl calc/meas	1.00330492E+00	1.00308309E+00	1.00318708E+00	1.00308385E+00	1.00304536E+00	1.00325501E+00

An explanation of atomic spectra begins with the ionization energies.

		CRC ionization energy (eV)				
H	1	13.598440				
He	2	24.587380	54.417760			
LI	3	5.391710	75.640090	122.454350		
Be	4	9.322690	18.211150	153.896200	217.718580	
B	5	8.298030	25.154840	37.930640	259.375210	340.225800

		ionization energy Vi(J)				
H	1	13.120000				
He	2	23.659217	52.480000			
LI	3	5.188175	72.784711	118.080000		
Be	4	8.970763	17.523687	148.086687	209.920000	
B	5	7.984783	24.205256	36.498775	249.583912	328.000000

In atoms with more than one proton, the discretely exact energy (in red) for elemental ionization energy above which the atom no longer exists, is equal to product of the square of the number of protons times the discretely exact value for the hydrogen ionization energy. The intermediate ionization energies (in blue) are equal to the CRC value divided by *omega-2*.

		ionization frequency				
H	1	3.280000E+15				
He	2	5.914804E+15	1.312000E+16			
LI	3	1.297044E+15	1.819618E+16	2.952000E+16		
Be	4	2.242691E+15	4.380922E+15	3.702167E+16	5.248000E+16	
B	5	1.996196E+15	6.051314E+15	9.124694E+15	6.239598E+16	8.200000E+16

The ionization frequency is equal to the product of the ionization energy and the Coulomb divided by the discrete Planck constant.

		ionization wave number				
H	1	1.093333E+07				
He	2	1.971601E+07	4.373333E+07			
LI	3	4.323479E+06	6.065393E+07	9.840000E+07		
Be	4	7.475636E+06	1.460307E+07	1.234056E+08	1.749333E+08	
B	5	6.653986E+06	2.017105E+07	3.041565E+07	2.079866E+08	2.733333E+08

The ionization wave number is equal to the ionization frequency divided by the photon velocity.

		calculated wavelength				
H	1	6.585366E-07				
He	2	5.072019E-08	2.286585E-08			
LI	3	2.312952E-07	1.648698E-08	1.016260E-08		
Be	4	1.337679E-07	6.847874E-08	8.103362E-09	5.716463E-09	
B	5	1.502859E-07	4.957601E-08	3.287782E-08	4.808002E-09	3.658537E-09

The photon wavelength is the inverse of the wave number.

		measured wavelength				
H	1	6.563000E-07				
He	2	4.477000E-07	6.864000E-07			
LI	3	6.710000E-07	4.974000E-07	4.275000E-07		
Be	4	4.573000E-07	5.060000E-07	6.565000E-07	6.971000E-07	
B	5	4.197000E-07	4.472000E-07	4.506000E-07	4.941000E-07	6.284000E-07

		measured/calculated	wavelength			
H	1	**0.996604**	**1.00340787**			
He	2	8.826860	30.018560			
LI	3	2.901055	30.169263	42.066000		
Be	4	3.418608	7.389155	81.015759	121.946027	
B	5	2.792678	9.020492	13.705290	102.766176	171.762667

The difference between the calculated and measured value for the hydrogen ionization energy, divided by the difference between the measured wavelength and calculated wavelength for hydrogen ionization is very nearly equal to the difference between the photon velocity and the speed of light.

$$\frac{13.634704/13.598440}{6.563000x10^{-7}/6.585366x10^{-7}} = \frac{1.003407}{1.002667} = 1.000739 \cong 1.000692 = \frac{300000000}{299792458}$$

The difference between these two values, independent of how it is calculated, is a measurement error term of approximately 0.00468%.

$$\frac{1.000739-1.000692}{1.000739} = .00468058\% \qquad \frac{1.000739-1.000692}{1.000692} = .00468080\%$$

The differences between the measured and calculated values for hydrogen are of no concern and, even though the Rydberg equations derive the measurable wavelengths to high accuracy, the explanation requiring the simultaneous emission of two photons is not consistent with the spectral mechanism hypothesis.

The Rydberg explanation for the emission of atomic spectra requires two frequencies:

- One frequency is the structural frequency. Structural frequency is proportional to the energy of the positional resonance between an electron and proton (the energy required to hold the electron and proton in the positional resonance).
- The photon frequency, equal to the difference between adjacent structural frequencies, is proportional to an ionization energy (the energy required to remove an electron from the positional resonance).

The photon frequency and wavelength are not directly proportional to structural energy and, in atoms larger than hydrogen, cannot be calculated by a Rydberg equation.

Proofs that wavelength and frequency are not directly proportional to energy:

- Spectral wavelengths emitted by sources differing greatly in energy, by a discharge tube in the laboratory, by the sun or by the galactic center, are indistinguishable.
- In 60 Hertz power transformers the energy of the emitted photons is proportional to the energy of the current (or the magnetic field).

A general explanation for atomic spectra requires an examination of the measured ionization energies and the measured wavelengths of the first four elements larger than hydrogen.

		CRC ionization energy (eV)				
H	1	13.598440				
He	2	24.587380	54.417760			
LI	3	5.391710	75.640090	122.454350		
Be	4	9.322690	18.211150	153.896200	217.718580	
B	5	8.298030	25.154840	37.930640	259.375210	340.225800

		Atomic intrinsic energy Vi(J)				
H	1	13.120000				
He	2	23.659217	52.480000			
LI	3	5.188175	72.784711	118.080000		
Be	4	8.970763	17.523687	148.086687	209.920000	
B	5	7.984783	24.205256	36.498775	249.583912	328.000000

		measured wavelength				
H	1	6.563000E-07				
He	2	4.477000E-07	6.864000E-07			
LI	3	6.710000E-07	4.974000E-07	4.275000E-07		
Be	4	4.573000E-07	5.060000E-07	6.565000E-07	6.971000E-07	
B	5	4.197000E-07	4.472000E-07	4.506000E-07	4.941000E-07	6.284000E-07

The number of CRC ionization energies (electron Volts in units of kinetic Joule) for each elemental atom larger than hydrogen is equal to the number of nuclear protons; and the number of atomic energies (intrinsic Volts in units of discrete Joule) is also equal to the number of nuclear protons.

While it is true that measured wavelengths are not directly proportional to energy, it is also true that shorter wavelengths are proportional to lower energies and longer wavelengths are proportional to higher energies. For example, ultraviolet photons have shorter wavelengths and lower energies, and visible photons have longer wavelengths and higher energies.

In any atomic spectrum, each measured wavelength corresponds to one specific energy and, in order for each measured wavelength to correspond to one specific energy, the number of wavelengths must either be equal to the number of energies or equal to an integer multiple of the number of energies.

For example, in helium there are two CRC ionization energies (electron Volts in units of kinetic Joule) corresponding to two atomic energies (intrinsic Volts in units of discrete Joule), fourteen measured wavelengths, and one transition between a wavelength proportional to a lower energy and a wavelength proportional to a higher energy.

In the below table, seven lower and seven higher helium atomic energies are in the first row, the measured wavelengths from shortest to longest are in the third row, and the second row is the ratio of the column wavelength divided by the adjacent lower wavelength. This is the definitive test for a transition from a wavelength corresponding to a lower energy to a wavelength corresponding to a higher energy. In the helium atom, the transition wavelength is also detectable by inspection of the previous wavelengths compared to the following wavelengths.

Helium														
Vi(J)	23.6592	23.6592	23.6592	23.6592	23.6592	23.6592	23.6592	52.4800	52.4800	52.4800	52.4800	52.4800	52.4800	52.4800
		1.0040	1.0228	1.0066	1.0583	1.0116	1.0081	1.0605	1.0381	1.0181	1.0062	1.1636	1.1357	1.0281
meas wl	40.1300	40.2900	41.2100	41.4800	43.9000	44.4100	44.7700	47.4800	49.2900	50.1800	50.4900	58.7500	66.7200	68.5976

The transitions are less clear in lithium, beryllium, and boron.

Lithium						
Vi(J)	5.1882	5.1882	72.7847	72.7847	118.0800	118.0800
		1.0344	1.0767	1.0806	1.2278	1.0987
meas wl	413.3000	427.5000	460.3000	497.4000	610.7000	671.0000

Beryllium												
Vi(J)	8.9708	8.9708	8.9708	17.5237	17.5237	17.5237	148.0867	148.0867	148.0867	209.9200	209.9200	209.9200
		1.0364	1.0367	1.0311	1.0295	1.0424	1.2316	1.0390	1.0139	1.0341	1.0138	1.0128
meas wl	425.6000	441.1000	457.3000	471.5000	485.4000	506.0000	623.2000	647.5000	656.5000	678.9000	688.3000	697.1000

Boron										
Vi(J)	7.9848	7.9848	24.2053	24.2053	36.4988	36.4988	249.5839	249.5839	328.0000	328.0000
		1.0172	1.0122	1.0527	1.0040	1.0036	1.0626	1.0320	1.2301	1.0339
meas wl	412.6000	419.7000	424.8000	447.2000	449.0000	450.6000	478.8000	494.1000	607.8000	628.4000

In lithium, beryllium and boron the transition wavelengths are not definitively detectable by simple inspection. However, after the higher energy transitions are established by the ratios of the column wavelength divided by the adjacent lower wavelength, the first transition becomes apparent by inspection of the measured wavelengths.

The spectral mechanism hypothesis has been transformed into a general explanation for atomic spectra:

In hydrogen a single electron and proton are engaged in a positional resonance at a discretely exact frequency equal to 3.28E15 Hz. In atoms larger than hydrogen many electrons and protons are engaged in sustained positional resonances, equal to the product of the square of the number of nuclear protons and 3.28E15 Hz, in which CCW quantons are emitted in one direction by electrons and absorbed by nuclear protons, and CW quantons are emitted in the opposite direction by nuclear protons and absorbed by electrons. The positional resonances can be situated at any one of several quantized positions proportional to energy and corresponding to spectral emission and absorption lines. On emission of a photon the energy of the resonance decreases, and the electron drops to a lower energy level. On absorption of a photon the energy of the resonance increases and the electron jumps to a higher energy level.

Part Six

Cosmology

The purpose of this chapter is to disprove cosmic inflation:

- The radiated intrinsic energy which drives the resonance of constant photon velocity is converted into units of intrinsic redshift per megaparsec.
- A detailed general derivation of intrinsic redshift (applicable to any galaxy) is made.
- The final results of the HST Key Project to measure the Hubble Constant are explained by intrinsic redshift.[22]

The only measurables in the determination of galactic redshifts are the photon wavelength emitted and received in the laboratory, the photon wavelength emitted by a galaxy and received by an observatory, and the ionization energies.

In the following equations Hydrogen-alpha (Balmer-A) wavelengths are used in calculations of intrinsic redshift.

Intrinsic redshift per megaparsec

The photon intrinsic energy radiated per second due to quanton/graviton emissions is equal to the product of 8 and the discrete Planck constant.

$$V_{i(J)radiated/s} = 8h = 5.3333333300x10^{-33} \ \left(\mathrm{J/s}\right)$$

The 2015 IAC value for the megaparsec is proportional to the IAC exact SI definition of the astronomical unit (149,597,870,700 m).

$$mpc = \frac{648000 \ x \ 14959787070 \ x \ 10^6}{\pi} = 3.08567758x10^{22} \ \left(\mathrm{m}\right)$$

The time of flight per megaparsec is equal to one mpc divided by the photon velocity.

$$tof \ / \ mpc = \frac{mpc}{c} = 1.02855919x10^{14} \ \left(\mathrm{s}\right)$$

[22] Final Results from the Hubble Space Telescope Key Project to Measure the Hubble Constant, Astrophysical Journal 0012-376v1, 18 Dec 2000.

The photon intrinsic energy radiated per megaparsec is equal to the product of time of flight per mpc and the photon intrinsic energy radiated per second due to quanton/graviton emissions.

$$V_{i(J)radiated} / mpc = (tof / mpc)\, x\left(V_{i(J)radiated/s}\right) = 5.4856490338x10^{-19} \ \ (\mathrm{J})$$

The decrease in photon frequency due to the energy radiated is equal to the photon intrinsic energy radiated per megaparsec divided by the discrete Planck constant.

$$f_{ph}decrease = \frac{V_{i(J)radiated}}{h} = 8.2284735506x10^{14} \ \ (\mathrm{Hz})$$

The increase in photon wavelength due to the photon intrinsic energy radiated is equal to the ratio of the photon velocity divided by decrease in photon frequency.

$$\lambda_{ph}increase = \frac{c}{f_{ph}decrease} = 3.6458767006x10^{-7} \ \ (\mathrm{m})$$

Note that wavelength and energy are independent thus wavelength cannot be directly determined from energy, but frequency is proportional to energy and the decrease in frequency is proportional to the increase in wavelength.

The intrinsic redshift per megaparsec is equal to the Hydrogen-alpha (Balmer-A) emission wavelength plus the wavelength increase.

$$z_i / mpc = \lambda_{ph}emitted + \lambda_{ph}increase = 1.0231242554x10^{-6} = 0.0000010231$$

General derivation of galactic intrinsic redshift

The distance of the galaxy in units of mpc is that determined by the Hubble Space Telescope Key Project.[23] Below, the example calculations are for NGC0300.

The time of flight of photons emitted by NGC0300 is equal to the product of the time of flight per megaparsec and the Hubble Space Telescope Key Project distance of the galaxy.

$$tof / d_{NGC0300} = \left(\frac{3.08567758x10^{22}}{c}\right) x\ d_{NGC0300} = 2.0776895715x10^{14} \ \ (\mathrm{s})$$

[23] Page 60, Final Results from the Hubble Space Telescope Key Project to Measure the Hubble Constant, Astrophysical Journal 0012-376v1, 18 Dec 2000.

The photon intrinsic energy radiated by NGC0300 is equal to the product of the time of flight at the distance of NGC0300 and the photon intrinsic energy radiated per second due to quanton/graviton emissions.

$$V_{i(J)radiated} / d_{NGC0300} = (tof / d_{NGC0300}) x (V_{i(J)radiated/s}) = 1.1081011048x10^{-18} \ (\mathrm{J})$$

The decrease in photon frequency is equal to the photon intrinsic energy radiated by NGC0300 divided by the discrete Planck constant.

$$f_{ph}decrease = \frac{V_{i(J)radiated} / d_{NGC0300}}{h} = 1.6621516572x10^{15} \ (\mathrm{Hz})$$

The increase in photon wavelength due to the photon intrinsic energy radiated is equal to the ratio of the photon velocity divided by decrease in photon frequency.

$$\lambda_{ph}increase = \frac{c}{f_{ph}decrease} = 1.8048894558x10^{-7} \ (\mathrm{m})$$

The intrinsic redshift at the distance of NGC0300 is equal to the Hydrogen-alpha (Balmer-A) emission wavelength plus the wavelength increase.

$$z_i / d_{NGC0300} = \lambda_{ph}emitted + \lambda_{ph}increase = 8.3902553094x10^{-7} = 0.0000008390$$

Results of the HST Key Project to measure the Hubble Constant

The goal of this massive international project, involving more than fifteen years of effort by hundreds of researchers, was to build an accurate distance scale for Cephied variables and use this information to determine the Hubble constant to an accuracy of 10%.

The inputs to the HST key project were the observed redshifts and the theoretical relativistic expansion rate of cosmic inflation.

In column 2 below, the galactic distances of 22 galaxies in units of mpc are the values determined by the HST Key Project.[24]

In column 3 below, the galactic distances are expressed in units of meter.

[24] Page 60, Final Results from the Hubble Space Telescope Key Project to Measure the Hubble Constant, Astrophysical Journal 0012-376v1, 18 Dec 2000.

In column 4 below, the time of flight of photons emitted by the galaxy is equal to the distance of the galaxy in meters divided by the photon velocity.

$$tof\ /\ d_{galaxy} = \frac{d_{galaxy}}{c}\ \left(\mathrm{s}\right)$$

Galaxy	dmpc	dm	tof	zi	Hubble
NGC 0300	2.020000	6.233069E+22	2.077690E+14	0.0000008390	308682.322
NGC 2403	3.130000	9.658171E+22	3.219390E+14	0.0000007750	199213.511
NGC 5253	3.250000	1.002845E+23	3.342817E+14	0.0000007707	191857.936
IC 4182	4.530000	1.397812E+23	4.659373E+14	0.0000007390	137646.422
NGC 0925	9.120000	2.814138E+23	9.380460E+14	0.0000006985	68370.427
NGC 3351	9.330000	2.878937E+23	9.596457E+14	0.0000006976	66831.542
NGC 3368	9.860000	3.042478E+23	1.014159E+15	0.0000006955	63239.178
NGC 2541	11.220000	3.462130E+23	1.154043E+15	0.0000006910	55573.823
NGC 2090	11.430000	3.526929E+23	1.175643E+15	0.0000006904	54552.781
NGC 4725	11.910000	3.675042E+23	1.225014E+15	0.0000006891	52354.181
NGC 3198	13.680000	4.221207E+23	1.407069E+15	0.0000006852	45580.284
NGC 4321	14.320000	4.418690E+23	1.472897E+15	0.0000006840	43543.177
NGC 4536	14.450000	4.458804E+23	1.486268E+15	0.0000006838	43151.439
NGC 7331	14.520000	4.480404E+23	1.493468E+15	0.0000006836	42943.408
NGC 4496A	14.520000	4.480404E+23	1.493468E+15	0.0000006836	42943.408
NGC 4535	14.790000	4.563717E+23	1.521239E+15	0.0000006832	42159.452
NGC 4548	15.000000	4.628516E+23	1.542839E+15	0.0000006828	41569.219
NGC 1326A	16.140000	4.980284E+23	1.660095E+15	0.0000006811	38633.104
NGC 4414	16.600000	5.122225E+23	1.707408E+15	0.0000006805	37562.548
NGC 1365	17.220000	5.313537E+23	1.771179E+15	0.0000006797	36210.121
NGC 1425	20.890000	6.445980E+23	2.148660E+15	0.0000006760	29848.650
NGC 4639	20.990000	6.476837E+23	2.158946E+15	0.0000006759	29706.445
				discrete calculated	76007.881
				HST 2000 value	78092.000

The photon intrinsic energy radiated due to quanton/graviton emissions at the distance of the galaxy is equal to the product of the time of flight of photons emitted by the galaxy and the photon intrinsic energy radiated per second.

$$V_{i(J)radiated}\ /\ d_{galaxy} = \left(tof\ /\ d_{galaxy}\right) x \left(V_{i(J)radiated/\mathrm{s}}\right)\ \left(\mathrm{J}\right)$$

The decrease in photon frequency is equal to the photon intrinsic energy radiated by the galaxy divided by the discrete Planck constant.

$$f_{ph}decrease = \frac{V_{i(J)radiated}\ /\ d_{galaxy}}{h}\ \left(\mathrm{Hz}\right)$$

The increase in photon wavelength due to the photon intrinsic energy radiated is equal to the ratio of the photon velocity divided by decrease in photon frequency.

$$\lambda_{ph} increase = \frac{c}{f_{ph} decrease} \ \left(\mathrm{m}\right)$$

Above column 5, the intrinsic redshift at the distance of the galaxy is equal to the Hydrogen-alpha (Balmer-A) emission wavelength plus the wavelength increase.

$$z_i / d_{galaxy} = \lambda_{ph} emitted + \lambda_{ph} increase$$

The Hubble parameter for a galaxy, equal to the product of the ratio of 2 *omega-2* (converts intrinsic energy to kinetic energy) divided by the time of flight of photons received at the observatory that were emitted by the galaxy, and the ratio of the distance of the galaxy in units of kilometer divided by the distance of the galaxy in units of megaparsec, is denominated in units of km/s per mpc.

$$\left(\frac{2\omega^2}{tof \ / d_{galaxy}}\right) x \left(\frac{d_{galaxy(km)}}{d_{galaxy(mpc)}}\right) = H_P \ \left(\frac{\mathrm{km/s}}{\mathrm{mpc}}\right)$$

The Hubble constant is equal to the sum of the Hubble parameters for the galaxies examined divided by the number of galaxies.

$$\left(\frac{\sum H_P}{\#\ \mathrm{galaxies}}\right) = H_0 \ \left(\frac{\mathrm{km}}{\mathrm{mps\ sec}}\right)$$

The theory of cosmic inflation has been disproved.

Part Seven

Magnetic levitation and suspension

This chapter was motivated by a video about quantum magnetic levitation and suspension in which superconducting disks containing thin films of YBCO are levitated and suspended on a track composed of neodymium magnet arrays in which a unit array contains four neodymium magnets (two diagonal magnets oriented N→S and the other two S→N).[25]

An understanding of levitation and suspension by neodymium magnet arrays begins with consideration of the differences between the levitation of a superconducting disk containing thin films of metal oxides and the levitation of thin slice of pyrolytic carbon.

Oxygen is paramagnetic. An oxygen atom is magnetized by the magnetic field of a permanent magnet in the direction of the external magnetic field (for example, a S→N external magnetic field induces a S→N internal field) and reverts to a demagnetized state when the field is removed. The levitation of a superconducting disk requires an array of neodymium magnets and cooling below the critical temperature. In quantum levitation or suspension, the position of the disk is established by holding (pinning) it in the desired location and orientation, and if a pinned disk is forced into a new location and orientation, it remains pinned in the new location.

Carbon is diamagnetic. A carbon atom is magnetized by a magnetic field in the direction opposite to the magnetic field (for example, a N→S external magnetic field induces a S→N internal field) and reverts to a demagnetized state when the field is removed. Magnetic levitation occurs at room temperature, a thin slice of pyrolytic carbon levitates at a fixed distance parallel to the surface of an array of neodymium magnets, and a levitated slice forced closer to the surface springs back to the fixed distance once the force is removed.

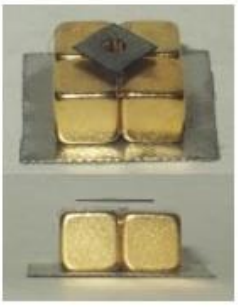

A small (~6mm) piece of pyrolytic graphite levitating over a permanent neodymium magnet array (5mm cubes on a piece of steel). Note that the poles of the magnets are aligned vertically and alternately (two with north facing up, and two with south facing up, diagonally)

Above, levitation of pyrolytic carbon.[26]

[25] "Dr. Boaz Almog: Quantum Levitation" https://www.youtube.com/watch?v=4HHJv8lPERQ .

[26] This image has been released into the public domain by its creator, Splarka. https://commons.wikimedia.org/wiki/File:Diamagnetic_graphite_levitation.jpg

In the levitation of pyrolytic carbon, CCW quantons are emitted by a magnetic North pole and CW quantons are emitted by a magnetic South pole (magnetic emission of quantons is discussed in Part Four).

The number of chirality meshing interactions required to exactly oppose the gravitational force on a thin slice of pyrolytic carbon (or any object) is equal to the local gravitational constant of earth divided by the product of the proton amplitude and the square root of *Lambda-bar*.

$$\text{levitation } \#CMIs = \frac{g_{\oplus}}{a_p \sqrt{\lambda\!\!\!^{-}}} = \sqrt[4]{48x10^{64}} = 2.632148x10^{16} \ \left(\text{Hz}\right)$$

In the above equation, the local gravitational constant of earth (as derived in Part One) is equal to 10 meters per second per second and the proton amplitude (also derived in Part One) is equal to 150 and, (as derived in Part Four) the square root of *Lambda-bar* is the deflection distance (units of meter) of a single chirality meshing interaction between a quanton and an electron.

The above equation is proportional to energy: the higher the energy, the higher the number of chirality meshing interactions, and the higher the levitation distance; the lower the energy, the lower the number of chirality meshing interactions, and the lower the levitation distance.

Pyrolytic carbon is composed of planar sheets of carbon atoms in which a unit cell is composed of a hexagon of carbon atoms joined by double bonds. Carbon atoms are bonded by either lower energy single bonds proportional to the first ionization energy or higher energy double bonds proportional to the second ionization energy. The measured first and second ionization energies of carbon are 1086.5 and 2352.0 (units of kJ/mol)[27].

Due to the discretely exact value of PE charge resonance, in carbon (or any elemental atom) the quanton emission-absorption frequency is equal to 3.28E15 Hz.

The quanton emission frequency of a unit cell of pyrolytic carbon is equal to the product of the discretely exact PE charge resonance frequency of 3.28E15 Hz and the ratio of the second ionization energy of carbon divided by the first ionization energy of carbon.

$$\text{emission frequency} = 3.28x10^{15} x\left(2352.0 \big/ 1086.5\right) = 7.100377x10^{15} \ \left(\text{Hz}\right)$$

The levitation distance of a thin slice of pyrolytic carbon (in units of mm) is equal to the product of the ratio of quanton emission frequency of a pyrolytic carbon unit cell divided by six (the number of carbon atoms in a unit cell) times 1000 mm/m and the square root of *Lambda-bar*.

$$\text{levitation distance} = \left(\frac{7.100377x10^{15}}{6}\right) x1000x\sqrt[4]{2.43x10^{70}} = 2.997289 \ \left[\text{mm}\right]$$

[27] Ionization energies of the elements (data page), https://en.wikipedia.org/

The oxygen atoms in YBCO oxides are bonded by either lower energy single bonds proportional to the first ionization energy or higher energy double bonds proportional to the second ionization energy. The measured first and second ionization energies of oxygen are 1313.9 and 3388.3 (units of kJ/mol).

The three YBCO metallic oxides are composed of low energy single bonds, high energy double bonds, or single and double bonds. In yttrium oxide (Y2O3), a single bond connects each yttrium atom with the inside oxygen, and a double bond connects each yttrium atom with one of the two outside oxygens. In barium oxide (BaO) the two atoms are connected by a double bond. Copper oxide is a mixture of cupric oxide (copper I oxide) in which a single bond connects each of two copper atoms with the oxygen atom, and cuprous oxide (copper II oxide) in which a double bond connects the copper atom with the oxygen atom.

Voltage is the emission of quantons either directly by the Q-axis of an electron or proton or transversely by a magnetic field from which CCW quantons are emitted by the North pole and CW quantons by the South pole.

The mechanism of magnetic levitation or suspension of a superconducting disk is the absorption of quantons, emitted by a neodymium magnet array, in chirality meshing interactions by electrons in the oxygen atoms of superconductingYBCO oxides resulting in repulsive deflections due to CCW quantons (in quantum levitation) and attractive deflections due to CW quantons (in quantum suspension).

The levitation or suspension distance of a superconductingYBCO oxide is higher (the maximum distance) for double bonded oxides and lower (the minimum distance) for single bonded oxides. The initial position of the YBCO disk is established by momentarily holding (pinning) it in the desired location and orientation at some specific distance from the neodymium magnet array.

In each one-hundredth of a second more than 2E14 chirality meshing interactions establishes the intrinsic energy of electrons within the superconducting oxides. At the same time, at any specific distance above or below the neodymium magnet array the number of quanton interactions, inversely proportional to the square of distance, establishes the availability of quantons to be absorbed at that specific distance. The result is an electrical Stable Balance of the electrons in superconducting oxides at specific distances from the neodymium magnet array, analogous to the gravitational Stable Balance of particles in planets at a specific orbital distance from the sun.

This is the mechanism of pinning in YBCO superconducting disks.

The levitation or suspension distance (units of mm) of a single bonded superconductingYBCO oxide is equal to the product of the ratio of the first ionization energy of oxygen divided by itself, the discretely exact PE charge resonance of 3.28E15 Hz, the square root of *Lambda-bar*, the ratio of the discrete steric factor divided by 1 (single bond), and 1000 (to convert m to mm).

$$\text{distance} = \left(1313.9/1313.9\right) x 3.28 x 10^{15} x \sqrt[4]{2.43 x 10^{70}}\, x \left(8/1\right) x 1000 = 66.460295 \ (\text{mm})$$

The levitation or suspension distance (units of mm) of a double bonded superconductingYBCO oxide is equal to the product of the ratio of the second ionization energy of oxygen divided by the first ionization energy of oxygen, the discretely exact PE charge resonance of 3.28E15 Hz, the square root of *Lambda-bar*, the ratio of the discrete steric factor divided by 2 (double bond), and 1000 (to convert m to mm).

$$\text{distance} = \left(3388.3 \middle/ 1313.9\right) x 3.28 x 10^{15} x \sqrt[4]{2.43 x 10^{70}}\, x \left(8 \middle/ 2\right) x 1000 = 85.694275 \ (\text{mm})$$